Food Hydrocolloids for Health 1 (2021) 100024

Contents lists available at ScienceDirect

Food Hydrocolloids for Health

journal homepage: www.elsevier.com/locate/fhfh

Formulation design, production and characterisation of solid lipid nanoparticles (SLN) and nanostructured lipid carriers (NLC) for the encapsulation of a model hydrophobic active

Georgia I. Sakellari[a,*], Ioanna Zafeiri[a], Hannah Batchelor[b], Fotis Spyropoulos[a]

[a] School of Chemical Engineering, University of Birmingham, Edgbaston, Birmingham, B15 2TT, UK
[b] Strathclyde Institute of Pharmacy and Biomedical Sciences, University of Strathclyde, 161 Cathedral Street, Glasgow, G4 0RE, UK

ARTICLE INFO

Keywords:
Solid lipid nanoparticles
Nanostructured lipid carriers
Hydrophobic active
Crystallinity
Pickering functionality
Hansen solubility parameter

ABSTRACT

Lipid nanoparticles have been widely investigated for their use as either carriers for poorly water soluble actives or as (Pickering) emulsion stabilisers. Recent studies have suggested that the fabrication of lipid nanostructures that can display both these performances concurrently, can enable the development of liquid formulations for multi-active encapsulation and release. Understanding the effects of different formulation variables on the microstructural attributes that underline both these functionalities is crucial in developing such lipid nanostructures. In this study, two types of lipid-based nanoparticles, solid lipid nanoparticles and nanostructured lipid carriers, were fabricated using varying formulation parameters, namely type of solid lipid, concentration of liquid lipid and type/concentration of surface active species. The impact of these formulation parameters on the size, thermal properties, encapsulation efficiency, loading capacity and long-term storage stability of the developed lipid systems, was studied. Preliminary lipid screening and processing conditions studies, focused on creating a suitable lipid host matrix of appropriate dimensions that could enable the high loading of a model hydrophobic active (curcumin). Informed by this, selected lipid nanostructures were then produced. These were characterised by encapsulation efficiency and loading capacity values as high as 99% and 5%, respectively, and particle dimensions within the desirable size range (100-200 nm) required to enable Pickering functionality. Compatibility between the lipid matrix components, and liquid lipid/active addition were shown to greatly influence the polymorphism/crystallinity of the fabricated particles, with the latter demonstrating a liquid lipid concentration-dependent behaviour. Successful long-term storage stability of up to 28 weeks was confirmed for certain formulations.

1. Introduction

Lipid nanoparticles comprise a widely used platform of lipid-based colloidal vehicles, as they have emerged into versatile nanocarriers due to their auspicious attributes in addressing issues commonly encountered with active encapsulation and delivery. These include solubility and bioavailability enhancement of poorly water soluble actives (Bunjes, 2010; Hu, Tang, & Cui, 2010; Pouton, 2006), as well as improved stability and shielding of actives prone to degradation (Sapino et al., 2005; Souto & Müller, 2005). Solid lipid nanoparticles (SLNs) and nanostructured lipid carriers (NLCs) are two types of nanoparticulate systems, that consist of a lipid core formed either of solid lipids (solid at room and body temperature), or mixtures with liquid lipids (liquid at room temperature), respectively, with the diversity in the fatty acid composition introduced by the latter allowing for quite large distances inside the matrix (Müller, Radtke, & Wissing, 2002). Both types of lipid nanostructures have been extensively investigated for their potential to function as delivery systems for a wide range of active ingredients, though current literature primarily focuses on the delivery of poorly water-soluble drugs and bioactive molecules (Borges et al., 2020; Jaiswal, Gidwani, & Vyas, 2016; Khan et al., 2015; Severino et al., 2012; Weiss et al., 2008). In the last decade, their range of applications has expanded to include their usage in Pickering emulsion stabilisation, principally due to their ability to provide sufficient emulsion stability (Gupta & Rousseau, 2012), and their inherent tuneable microstructure compared to conventional emulsifiers (Pawlik et al., 2016; Zafeiri et al., 2017a). Within the research area of combining the two functionalities, i.e. acting/serving as active carriers and providing emulsion stabilisation, SLNs have been successfully utilised for the two-fold purpose of encapsulating/controlling the release of a hydrophobic active and stabilising o/w or w/o emulsion droplets, both achieved by tuning their surface properties (Sakellari et al., 2021).

* Corresponding author.
E-mail address: gis823@bham.ac.uk (G.I. Sakellari).

https://doi.org/10.1016/j.fhfh.2021.100024
Received 31 May 2021; Received in revised form 5 August 2021; Accepted 20 August 2021

Despite the sheer number of studies investigating the structural properties of lipid particle dispersions regarding their use as active delivery systems, there is limited understanding on the correlation between such characteristics and the structures' capacity to afford effective Pickering stabilisation (Schröder et al., 2020). Among the attributes that have been reported to impact upon the Pickering stabilisation mechanism are the particle size and shape, surface properties, polymorphism and long-term (lipid particle) stability. The type of solid lipid and surfactant used during SLN fabrication has been shown to play a pivotal role in the long-term stabilisation of emulsion droplets (Zafeiri et al., 2017b). Nanoemulsion droplets with a volume-weighted mean particle diameter of 459 nm were stabilised by negatively charged glyceryl stearate citrate SLNs with a mean diameter of 152 nm for a period of 12 weeks (Gupta & Rousseau, 2012). Recently, Lim *et al.* (2020) studied the interfacial characteristics of tristearin SLNs in respect to the interfacial and colloidal stability of the SLN-stabilised emulsions, demonstrating that increasing the concentration of surfactant used in the SLN preparation, can prolong the stability of the attained emulsions (up to 1 month under the studied conditions). In another study, tailoring of submicron-sized particles, in terms of their crystalline structure and morphology, was achieved by alternating the lipid phase composition between tripalmitin, palm stearin or combination of tripalmitin and the liquid lipid tricaprylin (4:1 w/w), that resulted in varying emulsion stabilisation efficiency due to wettability and inter-particle interaction changes (Schröder et al., 2017).

The significance of the above properties and how they can be modulated to achieve desirable characteristics is not only limited to the development of lipid nanoparticle dispersions suitable for Pickering stabilisation. Crystalline structure properties have been investigated for their influence in addressing high active loading and resistance to drug leakage demands. The tendency of SLNs to transform into highly ordered structures and lead to active expulsion during storage has been addressed by partial substitution with incompatible liquid lipids (NLCs), to create imperfections in the lipid crystal lattice, that will in turn also accommodate higher active incorporation (Hu et al., 2005; Jia et al., 2010). The choice of the type and ratio between the solid and liquid lipids participating in such combinations can greatly affect the resulting lipid core organisation, while this can be further modified by the encapsulated molecule (Araujo et al., 2020; Bunjes et al., 2001; Jores, Mehnert, & Mäder, 2003). Compatibility between the lipid matrix components, affinity of the active for these, and contribution from the surfactant have been highlighted for their invariable association with high loading capacity, better controlled release performance, improved active bioavailability but also for their role in the final matrix arrangement (Anantachaisilp et al., 2010; Das & Chaudhury, 2011a; Kasongo et al., 2011a; Kovacevic et al., 2011; Müller, Mäder, & Gohla, 2000; Müller, Radtke, & Wissing, 2002; Obinu et al., 2020; Shah et al., 2012). The structural organisation of SLN and NLC lipid matrices has been a subject of debate, with numerous reports in literature utilising a range of structural and imaging techniques to determine the positioning of the solid lipid, liquid lipid and active components (Bunjes et al., 2001; Jenning, Thünemann, & Gohla, 2000b; Jores, Mehnert, & Mäder, 2003; Jores et al., 2004; Müller, Mäder, & Gohla, 2000; Müller, Radtke, & Wissing, 2002; Wolska et al., 2020). Oehlke *et al.* (2017) proposed the presence of the lipophilic tocopherol in the lipid matrix near the tail of the surfactant, as opposed to the location of the hydrophilic ferulic acid in the headgroup region, with the location of the former explaining the greater impact on halting prolonged melting behaviour changes. The effect of the relative affinity between the encapsulated active and the lipid used was demonstrated by the higher loading and slower release of the drug diclofenac from lipid particles containing high ratio of the solid lipid Gelucire® 50/13 compared to the drug dexamethasone, while faster release for both drugs was recorded when a partially miscible solid lipid (Witepsol® S55) and a liquid lipid (Capryol® 90) were added in the lipid matrix that was attributed to the creation of a less ordered crystalline state (Zoubari et al., 2017). Thus, understanding how and to what extent certain composition factors, including the gradual addition of liquid lipid and/or active, influence the structure of the solid lipid matrix can potentially provide further insight on how to form lipid particles with customised properties tailored to their intended functionalities and applications.

The present work aims to investigate the impact of formulation variables, including the incorporation of curcumin used as a model hydrophobic active, on specific physical characteristics of SLNs and NLCs. Curcumin is a lipophilic polyphenolic compound, widely studied by the pharmaceutical, cosmetic and food sectors due to its numerous attributes, including but not limited to anti-inflammatory, antimicrobial, anticancer and antioxidant properties (Sharifi-Rad et al., 2020). Similarly to other hydrophobic actives, curcumin requires the use of a suitable carrier, among which are lipid-based systems, to enhance its bioavailability and harness its health benefits (Anand et al., 2007), and thus it has been previously employed as a model hydrophobic active during the development of delivery systems (Khan et al., 2017; Scomoroscenco et al., 2021). The selection of lipid components (solid and liquid lipids) with high compatibility towards one another, that also show affinity for curcumin, was one of the primary focuses of the early development stages, towards the creation of a lipid core that can achieve high active entrapment and long-term physical integrity. For this purpose, theoretical predictions using the Hansen solubility parameter and experimental lipid screening studies were performed for both solid and liquid lipids, along with miscibility studies. Thereafter, lipid dispersions of both SLNs and NLCs were fabricated via a melt-emulsification-ultrasonication method in the presence of surface active species. Two types of solid lipids (singly or as blends), varying concentration of the liquid lipid and type/concentration of the surface active species were evaluated. The effect of these parameters on physical markers linked to Pickering functionality, that herein was confined in terms of appropriate size, together with the thermal properties, loading capacity and long-term storage stability of the lipid nanoparticles were assessed. Lipid screening as a formulation development aspect, and alterations in the formulation variables of the lipid nanoparticles have been previously studied individually towards the creation of systems with optimised properties. However, there has been a lack of cumulative investigation of the impact of these formulation aspects on the physical characteristics of particles fabricated under consistent processing parameters, where the novelty of the current study lies. Thus, it is envisaged that through this comprehensive study, gaining a better insight on the reliance between formulation composition and crystalline structure properties of the SLNs and NLCs will eventually allow for tuning of the release profiles of the encapsulated actives, without compromising the microstructural attributes that enable their Pickering functionality.

2. Materials and Methods

2.1. Materials

Glyceryl behenate (Compritol® 888 ATO), glyceryl palmitostearate (Precirol® ATO 5), linoleoyl polyoxyl-6-glycerides (Labrafil® M 2125 CS), propylene glycol dicaprolate/dicaprate (Labrafac™ PG), cetyl palmitate and lauroyl polyoxyl-32 glycerides (Gelucire® 44/14) were kindly provided from Gattefossé (Saint-Priest, France). Glyceryl monostearate (Imwitor® 960K), glyceryl citrate/lactate/linoleate/oleate (Imwitor® 375) and medium chain triglycerides (MCTs) (Miglyol® 812), microcrystalline glyceryl tristearate (Dynasan® 118) were a kind gift from IOI Oleo (IOI Oleochemicals GmbH, Germany). Polyoxyethylene sorbitan monooleate (Tween® 80), Poloxamer 188 (Pluronic® F-68), poly(vinyl alcohol) (PVA, MW 89,000-98,000), castor oil and curcumin (≥65%, HPLC) were purchased from Sigma-Aldrich (Sigma-Aldrich, UK). All chemicals were used without further purification. Double distilled water from Milli-Q systems (Millipore, Watford, UK) was used for all experiments.

2.2. Lipid screening

Lipid screening was performed to evaluate the solubility of curcumin, the chosen model hydrophobic active, in a variety of solid and liquid lipids, a parameter of critical importance in the formulation development process. In this study, the solubilisation capacity of various lipids towards curcumin was assessed through both theoretical and experimental lipid screening.

2.2.1. Theoretical lipid screening

Theoretical predictions regarding the compatibility between the selected active and different solid and liquid lipids were based on calculations of the Hansen solubility parameter (HSP). For this purpose, the lipids were treated as the organic "solvents" and curcumin was the organic active under investigation. According to the theory proposed by Hansen (2007), the total cohesion energy in an organic molecule is the sum of three individual energy sources arising from nonpolar, polar and hydrogen bonding interactions. Thus, the solubility parameter (δ) of a substance can be decomposed into three distinct components. The partial HSP parameters account for the aforementioned dispersion interactions (δ_D), permanent dipole-permanent dipole forces (δ_P) and hydrogen bonding (δ_H), measured in $MPa^{1/2}$.

HSPs for curcumin and a variety of solid and liquid lipids were calculated as follows:

$$\delta_D = \frac{\sum_i F_{di}}{V_m} \quad (1)$$

$$\delta_P = \frac{\sqrt{\sum_i F_{pi}^2}}{V_m} \quad (2)$$

$$\delta_H = \sqrt{\frac{\sum_i E_{hi}}{V_m}} \quad (3)$$

$$\delta = \sqrt{\left(\delta_D^2 + \delta_P^2 + \delta_H^2\right)} \quad (4)$$

where F_d, F_p, E_h denote the group contribution parameters associated with the dispersion and polar forces, and hydrogen bonding energy that characterise each functional group of the molecular structure, respectively, and V_m represents the molar volume. The group contribution values used for the calculations were in accordance with the work published by van Krevelen *et al.* (2009). Curcumin can exist in two tautomeric forms; a diketo and an enol conformation, which have relative ratios that vary depending on the temperature, solvent polarity, pH and aromatic ring substitution (Lee et al., 2013). Therefore, the solubility screening was performed for both tautomeric forms. Depending on the chemical composition of each lipid (*Table S1*), the total and individual HSP for each constituent were estimated. An example of the calculations performed can be found in the *Supplementary Information*. For lipids with clearly defined chemical composition and consistency, HSPs were calculated for each of their components and an overall parameter was then obtained based on molar weighted averages (*Table 1*). For the solid lipid Imwitor® 960K and the liquid lipids Labrafil® M 2125 CS and Imwitor® 375, where an exact composition was not provided by the manufacturer (*Table S2*), calculations were carried out using available information about the lipid component composition and making assumptions for the potential consistency combinations; in this case HSPs are displayed as averages (*Table 1* & *Fig. 1*), rather than absolute values.

The miscibility between two substances can be visualised using the three partial solubility parameters, acting as coordinates in a three-dimensional space developed by Hansen (HSP 3D space). The close proximity of two points, each corresponding to a different material, can be used as a measure of high interactions and miscibility occurrence. The modified difference between the HSP of the active (A) and a given lipid (B) (R_a), representing the distance between the two substances A and B in the HSP 3D space, was determined as follows:

$$R_a = \sqrt{4\left(\delta_{DA} - \delta_{DB}\right)^2 + \left(\delta_{PA} - \delta_{PB}\right)^2 + \left(\delta_{HA} - \delta_{HB}\right)^2} \quad (5)$$

Table 1
Theoretical and experimental solubility screening of curcumin (CRM) in different solid and liquid lipids.

	Compound name	δ_D	δ_P	δ_H	δ	*Ra* (diketo form)	*Ra* (enol form)	$\Delta\delta$ (diketo form)	$\Delta\delta$ (enol form)	*S*[*]
	CRM Diketo form	17.17	5.47	12.33	21.83					
	CRM Enol form	16.80	5.54	14.16	22.66					
Solid lipids	Compritol® 888 ATO	16.87	1.75	7.31	18.47	6.27	7.83	3.36	4.19	+
	Precirol® ATO 5	16.89	2.18	7.87	18.76	5.57	7.14	3.07	3.90	+
	Dynasan® 118	16.70	1.53	5.96	17.80	7.54	9.13	7.50	9.13	-
	Cetyl palmitate	16.42	0.89	3.56	16.82	10.00	11.60	5.01	5.84	-
	Imwitor® 960K[**]	16.96 ± 0.04	2.39 ± 0.16	8.64 ± 1.08	19.20 ± 0.54	4.85 ± 0.92	6.37 ± 1.00	2.63 ± 0.54	3.47 ± 0.54	-
Liquid lipids	Labrafac™ PG	17.04	4.10	7.30	18.99	2.94	3.77	5.15	6.68	+
	Labrafil® M 2125 CS[**]	16.75 ± 0.13	2.74 ± 0.61	8.13 ± 1.72	18.89 ± 0.90	5.15 ± 1.64	6.68 ± 1.73	2.94 ± 0.90	3.77 ± 0.90	+
	Imwitor® 375[**]	16.11 ± 6.68	6.42 ± 4.73	13.80 ± 8.24	22.42 ± 11.11	14.34 ± 8.43	14.11 ± 8.52	-0.59 ± 11.11	0.24 ± 11.11	+
	Miglyol® 812	16.65	2.86	6.38	18.06	6.57	8.23	3.77	4.61	+
	Castor oil	16.94	2.23	9.03	19.32	4.65	6.11	2.51	3.34	+

[*] *S* represents the solubility of 0.5% w/w curcumin. (+) indicates successful, while (-) indicates unsuccessful solubilisation after 1 h.
[**] For lipids that the exact composition was unknown the average values are reported after accounting for all possible combinations, and each calculated value is presented with its respective standard deviation.

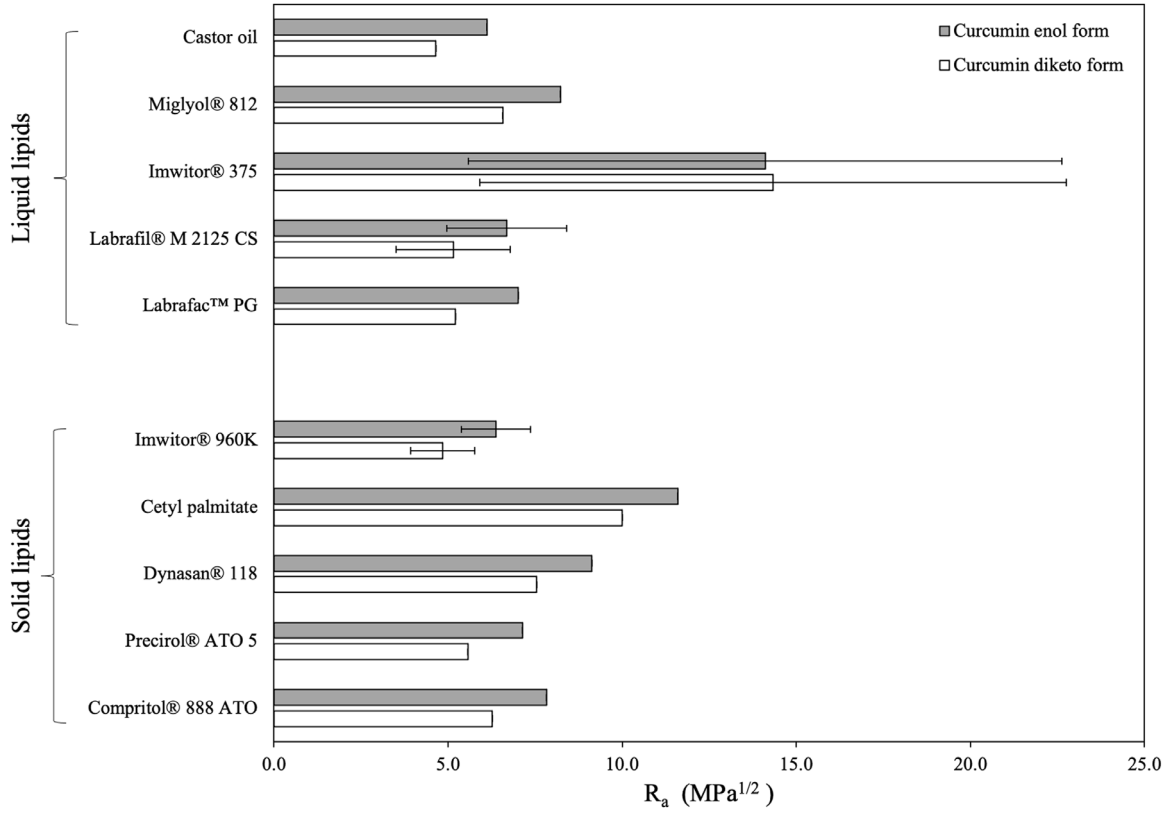

Fig. 1. Modified difference (R_a) between the two tautomeric forms of curcumin and various solid and liquid lipids. For lipids that the exact composition was unknown, the average *R*a value is reported after accounting for all possible combinations, and the error bars represent the standard deviation.

For a combination of miscible substances, the distance R_a should not exceed the radius of interaction (R_0), which gives the maximum difference allowed to define affinity between the active and a chosen solvent. The R_0 for the studied active can be found empirically using *Equation* 5 for a series of solvents with experimentally known HSPs (Hansen, 2007). More specifically, the solvents known to have good solubilisation capacity for curcumin and thus used in this study were propanone, ethyl ethanoate, n-butanol, methanol, ethanol and isopropanol (*Table S2*).

2.2.2. Experimental lipid screening

a. Selection of solid lipids. The maximum amount of curcumin that can be dissolved in 1 g of each solid lipid (Compritol® 888 ATO, Precirol® ATO 5, Dynasan® 118, cetyl palmitate, Imwitor® 960K) was determined by adding stepwise increasing amount of the active (1-2 mg) into the solid lipids. In order to mimic the experimental conditions followed for the lipid dispersions production (*Section 2.3*), each mixture was thermostatically maintained at 5-10°C above the melting point of each solid lipid, and let to stir for 1 h. The solubilisation of curcumin was evaluated by visual observation of formation of transparent homogeneous solutions with no visible traces of active crystals (Doktorovova, Souto, & Silva, 2017). The mixtures were left to cool down and stored in the dark at room temperature until further analysis.

b. Selection of liquid lipids. The choice of the liquid lipid used for the NLC dispersions was based on their ability to solubilise curcumin. A series of liquid lipids (Labrafil® M 2125 CS, Labrafac™ PG, Imwitor® 375, Miglyol® 812, castor oil) were tested, by adding increasing amount of the active (1-2 mg) in 1 g of each liquid lipid thermostated at 85°C and let to stir for 1 h, to simulate the process followed for the preparation of the lipid particle dispersions (*Section 2.3*). Similarly to the method described above for the selection of solid lipids, the solubilising power of each liquid lipid towards curcumin was assessed on their capacity to form transparent mixtures (Nnamani et al., 2014).

c. Miscibility of solid and liquid lipid systems. Blends of the solid and liquid lipids displaying the highest solubilising power towards curcumin were prepared in fractions, chosen based on the minimum and maximum amount of liquid lipid that was going to be used for the lipid dispersion fabrication, to examine their miscibility. The two solid lipids were mixed at a 50:50 w/w ratio, while 30% w/w of the solid lipid or solid lipid mixture was substituted by the liquid lipid for the blends containing both types of lipids. Curcumin was dissolved at 0.5% w/w of the total sample mass. The samples were agitated for 1 h at a temperature 5-10°C higher than the melting point of the solid lipids, to prepare the tempered solid lipids and blends of lipids, and then allowed to cool down at room temperature. The compatibility between the components was evaluated by both visual inspection for signs of turbidity or phase separation, coupled with differential scanning calorimetry (DSC, Setaram μDSC3 evo microcalorimeter, Setaram Instrumentation, France) analysis (Kasongo et al., 2011a). Specifically, the thermograms of the physical mixtures between the solid and liquid lipids with or without curcumin were compared to the thermograms of the respective tempered solid lipid.

2.3. Preparation of SLN and NLC aqueous dispersions

Blank and curcumin-loaded solid lipid nanoparticles and nanostructured lipid carriers (denoted as B-SLN or B-NLC and SLN or NLC, respectively) were prepared by a melt-emulsification-ultrasonication method, that has been previously described elsewhere (Zafeiri et al., 2017a). In brief, 2.5% of the lipid phase relating to the total mass (% w/w) was heated 5-10°C above the melting point of the lipid to ensure complete melting, and the heating state was maintained for approximately 1 h

to avoid lipid thermal memory effects (Van Malssen et al., 1996). More specifically, Compritol® 888 ATO and Precirol® ATO 5 were heated up to 85 and 70°C, respectively, and their 1:1 mixture was melted to around 85°C. When curcumin-loaded lipid particles were prepared, curcumin (0.5% w/w of the lipid mass) was added to the lipid phase and kept under magnetic stirring, until the active was completely dissolved (~1 h). The concentration of curcumin used was based on preliminary lipid screening studies. The temperature was monitored using a digital thermometer throughout all processes. For the NLCs, the liquid lipid concentrations used were 10, 20, or 30% of the total lipid content. The surfactant, Tween® 80 or Pluronic® F-68 (1.2 or 0.5% w/w of the total mass), was dissolved in the aqueous phase, which was heated to the same temperature as the molten lipid phase. The two phases were mixed by adding the aqueous to the lipid phase, and the mixture was stirred with a magnetic stirring bar for 15 minutes. The pre-emulsion was then homogenised using a high intensity ultrasonic Vibra-cell™ VC 505 processor (Sonics & Materials, Inc., CT, USA), operating continuously at 750 Watt and 20 kHz, at a sonication amplitude of 95% of the total power over a period of 5 minutes. To obtain the solid lipid particles, the o/w emulsion was subsequently cooled using an ice bath to a temperature below the crystallisation point of the lipid or mixture of lipids (1-4°C), with a cooling rate ranging between 0.5 and 2°C/min. Samples were stored at 4°C protected from light (since curcumin is photodegradable) until further analysis.

2.4. Physicochemical characterisation

2.4.1. Particle size, polydispersity and zeta potential analyses

Particle size and size distribution profiles were assessed either by dynamic light scattering (DLS) using a Zetasizer Nano ZS (Malvern Instruments, UK), or laser diffraction (LD) using a Mastersizer 2000 (Malvern Instruments, UK). For DLS measurements, the mean particle size (*Z*-average) was determined at a backscattering angle of 173° at 25°C. Polydispersity index (PDI) and zeta potential (ζ-potential) were additionally measured. All samples were appropriately diluted to avoid multiple scattering phenomena. In the case of LD, the samples were diluted with distilled water and stirred at 1200 rpm until an obscuration rate of approximately 5% was obtained. The mean diameters $D_{3,2}$ and span values were acquired to confirm signs of particle aggregation suggested by DLS measurements. The refractive indices of the materials used throughout the experiments were 1.55 for Compritol® 888 ATO and Precirol® ATO 5, 1.52 for their mixtures with Miglyol® 812, 1.52 for their 1:1 w/w mixture, 1.50 for their ternary mixture with Miglyol® 812 and 1.33 for distilled water. The absorption index was set at 0.01. Results are presented as the average value of 6 measurements with standard deviation (± S.D.).

2.4.2. Thermal analysis

Thermal analysis of the bulk materials and dispersions of lipid particles was carried out using a Setaram μDSC3 evo microcalorimeter (Setaram Instrumentation, France). Samples were accurately weighted (approximately 6.5 mg of bulk lipids or lipid mixtures and 600 mg of the lipid dispersions) and scanned between 20 and 90°C at a heating rate of 1.2°C/min, followed by a cooling cycle from 90 to 5°C. DSC data were used to investigate the compatibility of the lipid mixtures, the solid state of the cooled samples and the melting and crystallisation behaviour of the lipid dispersions. For bulk lipids, thermograms were obtained before and after tempering the lipids for 1 h at a temperature 5-10°C above their melting point. Information about the enthalpy, onset and peak temperatures was acquired through the Calisto Processing software. The DSC thermogram of pure curcumin was obtained using a DSC 25 (TA Instruments®, FR), where the sample was heated inside a Tzero® Hermetic Aluminum pan. The physical mixtures containing curcumin were additionally studied using the same equipment to investigate the presence or absence of crystalline curcumin by achieving higher temperature range. The temperature ramp used was 25 to 200°C at 5°C/min, with an empty pan used as reference. All enthalpy values and thermograms reported, are normalised for the amount of crystallising material present in the samples.

The degree of crystallinity was determined using the enthalpy derived from DSC data for the lipid nanoparticle dispersions and the lipid physical mixtures, and expressed by means of the recrystallisation indices (RI) which were calculated following the equation (Freitas & Müller, 1999):

$$RI = \frac{\Delta H_{SLN,\ NLC}}{\Delta H_{b.l.} \times C_{l.p.}} \times 100\ (\%) \quad (6)$$

where $\Delta H_{SLN,\ NLC}$ and $\Delta H_{b.l}$ represent the molar melting enthalpy (J/g) of the SLN and NLC aqueous dispersions and the bulk lipid phase respectively, and $C_{l.p.}$ is the % w/w concentration of the lipid phase.

2.4.3. Encapsulation efficiency and loading capacity

The entrapment efficiency (EE) and loading capacity (LC) were determined by ultrafiltration using centrifugal ultrafiltration tubes (Amicon® Ultra-4 filter 10 kDa cut-off, Millipore, Billerica, MA, USA). 1 mL of the curcumin-loaded lipid dispersions was added to the upper chamber of the centrifugal tube and centrifuged at 2,400 rcf for 1 h at room temperature using a SIGMA 3K-30 centrifuge (SciQuip®, UK). The concentration of unentrapped curcumin in the filtrate was subsequently determined by measuring the UV absorbance (Orion AquaMate 8000, Thermo-Scientific®, UK) at 425 nm, using a calibration curve that has been previously generated with linearity studied for 0-6 μg/mL and linear regression value of $R^2 = 0.9995$. The EE and LC were calculated using the following equations:

$$EE = \frac{W_{i.\ CRM} - W_{u.\ CRM}}{W_{i.\ CRM}} \times 100(\%) \quad (7)$$

$$LC = \frac{W_{i.\ CRM} - W_{u.\ CRM}}{W_{l.p.}} \times 100(\%) \quad (8)$$

where $W_{i.\ CRM}$ is the amount of curcumin that was initially used during the preparation of the aqueous lipid dispersions, $W_{u.\ CRM}$ is the amount of curcumin measured in the filtrate and $W_{l.p.}$ is the total amount of the lipid components used in the dispersions.

2.4.4. Assessment of storage stability

Stability studies of the aqueous SLN and NLC dispersions were performed over a period of 28 weeks with interval measurements performed at 1, 4 and 16 weeks, for samples stored at 4°C by measuring *Z*-average, PDI and ζ-potential. Changes in the physical state of the samples indicating destabilisation were assessed by visual inspection. Thermal behaviour and encapsulation efficiency were also evaluated over the same period.

2.5. Statistical analysis

Samples were prepared in at least duplicates and measurements were performed in at least triplicate and averages are reported with standard deviation. Figures depict the calculated average with error bars showing the standard deviation above and below the average. Comparison of means was conducted by ANOVA analysis followed by an all pairwise multiple comparison test using the Student-Newman-Keuls Method (SigmaPlot 14.5). The differences were considered statistically significant when $p < 0.05$.

3. Results and Discussion

3.1. Theoretical and experimental lipid screening

Using the Hansen solubility approach, theoretical predictions regarding the solubility of curcumin in different solid and liquid lipids, as well as their mixtures were performed. Based on that, materials with similar

solubility parameters will be miscible and in extend, actives will have a high affinity for lipids that are characterised by closely matching HSPs, leading to improved dispersion. This approach has been previously employed for the prediction of the miscibility between actives and different types of solid and liquid lipids (Shah & Agrawal, 2012), in combination with experimental screening in some instances (Doktorovova, Souto, & Silva, 2017; Kovačević, Müller, & Keck, 2020; Makoni et al., 2020; Shah & Agrawal, 2013), in order to identify the most suitable lipid-based solvent.

Comparing the intermolecular interactions between curcumin and the lipids under examination, shows that these mainly differ in their polar (δ_P) and hydrogen bonding (δ_H) forces, while the variance between the dispersion (δ_D) interactions was of smaller magnitude (*Table 1*). The smaller difference in the Hansen solubility parameter ($\Delta\delta$) between the active and the individual components of the lipids was observed for glyceryl mono-substituted esters (*Table 1* & *Fig. S1*). The presence of hydroxyl groups in the backbone of the glyceryl and polyethylenglycols (PEG) moieties could account for polar and hydrogen bonding interactions of higher strength with the hydroxyl groups of curcumin, explaining the aforementioned affinity. Exceptions to this observation were glyceryl monocitrate and glyceryl monolactate, components of Imwitor® 375, that were characterised by vastly different partial HSPs to those of curcumin, owing to the carboxylic acid and hydroxyl groups, respectively, present in their structure giving rise to significantly higher δ_P and δ_H values. The affinity of curcumin for di- and tri-substituted esters of glyceryl and polyethylenglycols was considerably lower. Similar results for curcumin have been reported previously by Doktorovova *et al.* (2017), but also for other actives showing increased affinity for monoglycerides compared to di- and triglycerides (Kovačević, Müller, & Keck, 2020; Makoni et al., 2020). Employing the calculated distance (R_a) in the Hansen 3D space, between curcumin and the various lipids, further confirmation about the greater solubilisation capacity of lipids containing higher percentage of monoglycerides (Compritol® 888 ATO, Precirol® ATO 5, Imwitor® 960K) was provided, on the basis that as the distance between them gets smaller, the miscibility increases (*Fig. 1*). Regarding the liquid lipids, Labrafac™ PG and castor oil displayed the smallest R_a values for either tautomeric forms. In their majority, liquid lipids were found to possess smaller R_a values than those of the solid lipids.

Experimental lipid screening data revealed that among all lipids, only Dynasan® 118, cetyl palmitate and Imwitor® 960K were not able to solubilise 0.5% w/w of the active (*Table 1*). Compritol® 888 ATO and Precirol® ATO 5 were the solid lipids that exhibited the highest curcumin solubility, approximately 0.6 and 0.7% w/w, respectively, which was in accordance with the theoretical predictions. For the liquid lipids Miglyol® 812 and Labrafil® M 2125 CS, this was close to 1% w/w. Overall, good agreement between theoretical and experimental results was observed, with a certain inconsistency for Imwitor® 960K. The percentage of monoglycerides in the specific lipid was the highest between the solid lipids, and thus it would be expected to show high affinity for curcumin. However, since the precise consistency of the lipids was unspecified and the theoretical predictions were based on average values resulting from different consistency combinations, the HSPs reported here could only be seen as approximations of the true values. Accordingly, data for Imwitor® 375 and Labrafil® M 2125 CS should be viewed in the same way. Another observation made regarding the HSP predictions was that correlation between the calculated R_a and R_0 (8.01 for the diketo and 7.41 for the enol form), suggests that most lipids (except cetyl palmitate) are expected to solubilise curcumin, since their R_a values were smaller than the radius of interaction, as suggested previously in literature (Doktorovova, Souto & Silva, 2017). A possible explanation could be given by the fact that the R_0 used here was deducted employing substances that are known to display relatively high curcumin affinity. Including solvents with a wider range of HSPs could have impacted the predictions, and therefore, while HSPs calculated here offer an adequate approach for comparisons between the lipids, they should not be regarded as an actual measure of solvent solubility.

Finally, the theoretical solubility predictions, that were earlier performed to predict the compatibility of CRM with different lipids, were subsequently also applied to gain further insight into the miscibility between Compritol® 888 ATO and Precirol® ATO 5, and MCTs. The lipid used in the smaller proportion (Miglyol® 812) in the lipid matrix was treated as an "active", and glyceryl behenate and glyceryl palmitostearate as the "solvents" under investigation. Based on their Hansen solubility parameter difference, it was shown that MCTs have theoretically a higher compatibility with glyceryl behenate ($\Delta\delta = 0.42$) compared to glyceryl palmitostearate ($\Delta\delta = 0.71$). Kovacevic *et al.* (2011) and Araujo *et al.* (2020) briefly raised the importance of the lipid chemical nature, and solid-to-liquid lipid compatibility regarding their performance in relation to the location of the liquid fraction within the lipid matrix. The location of the liquid lipid in the crystalline matrix could also dictate the positioning of the hydrophobic active, as a result of the relatively higher affinity of hydrophobic actives for liquid lipids compared to solid lipids, and thus information about the former could provide performance prediction capabilities for the latter.

In view of both theoretical and experimental lipid screening, the solid lipids chosen to progress to the next steps of the investigation were Compritol® 888 ATO and Precirol® ATO 5, while Miglyol® 812 was used as the liquid lipid in further experiments. Among the liquid lipids that were evaluated, Miglyol® 812 showed the highest capacity to solubilise curcumin based on both theoretical and experimental screening data. Mixtures of these lipids, that contain fatty acids of vastly different alkyl chain lengths, could potentially accommodate higher active loading capacities, due to the presence of imperfections in the formed matrices (Müller, Radtke, & Wissing, 2002). The curcumin concentration, for both the physical mixtures and the lipid nanoparticle dispersions preparation, was fixed at 0.5% w/w (mass of active over mass of lipid content), which was within the solubilisation capacity limits for all selected lipids.

3.2 Thermal analysis of bulk lipids and their mixtures

Initial assessment was performed by visual observation, that indicated good compatibility for both binary and ternary lipid mixtures, as there were no signs of separation or turbidity inspected. For the samples containing curcumin, the mixtures appeared homogeneous and transparent while melting, forming limpid blends after solidification without any evidence of sedimented curcumin crystals. The heating thermogram of pure curcumin revealed a single endothermic peak at 180.1°C (*Fig. S2*). Absence of crystalline curcumin in the physical lipid mixtures was confirmed by their thermograms, with all identified thermal events being ascribed to the lipid components (*Fig. S3*). DSC analysis provided further information about the thermal behaviour of the mixtures, in regard to changes in their lipid composition or addition of curcumin, and the melting and crystallisation thermograms are presented in *Fig. 2*.

The heating thermogram of bulk Compritol® 888 ATO shows a single endothermic peak at 71.9°C (*Fig. 2A*), which has been previously assigned to a mixture of metastable polymorphic forms (Souto, Mehnert, & Müller, 2006). Glyceryl behenate is a mixture of variable triacylglycerols (TAG), containing glyceryl mono-, di- and tribehenates, for which the transition rate from α to β via β' is known to be dependent on the degree of homogeneity (Bayés-García, Sato, & Ueno, 2020). Pivette *et al.* (2014) demonstrated, after studying the polymorphism of the main components, separately and in proportions that correspond to the composition of glyceryl behenate, that this endothermic event can be attributed to α and sub-α or β' forms of mono-, di- and tribehenin. Regarding glyceryl behenate's re-crystallisation behaviour, the bulk and tempered lipids showed a single major exothermic peak at 70.2°C with a shoulder appearing at 71.1°C, both attributed to crystallisation of α forms, and a more pronounced at 66.1°C, relating to either a sub-α subcell or a β' transition (*Fig. 2B*) (Brubach et al., 2007). A level of re-

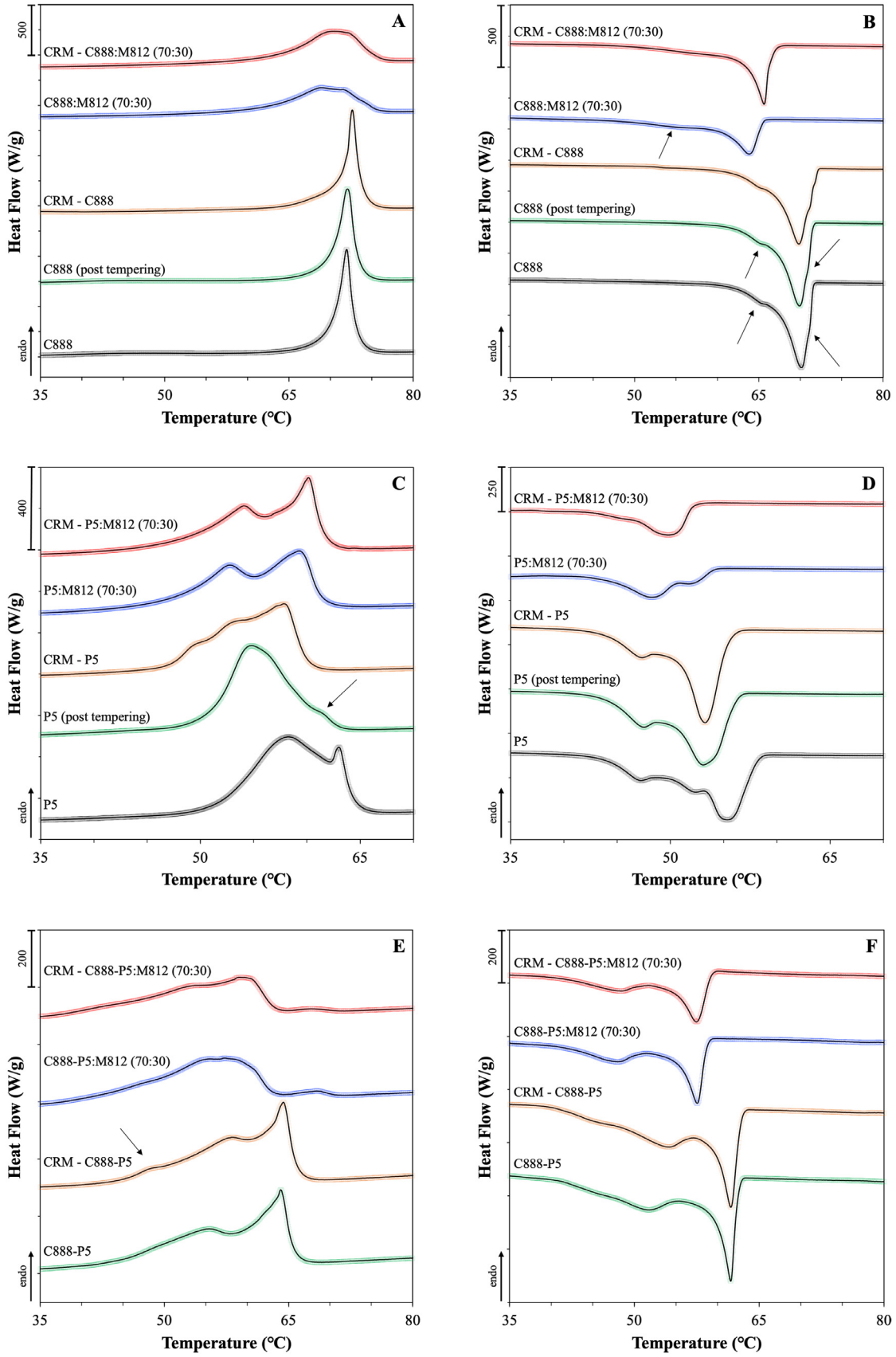

Fig. 2. DSC curves of binary and ternary solid and liquid lipid mixtures with or without curcumin (CRM, 0.5% w/w), consisting of Miglyol® 812 (M812) as the liquid lipid in combination with different solid lipids or blends of them. The melting and crystallisation thermograms presented in pairs are (A) and (B) for Compritol® 888 ATO (C888), (C) and (D) for Precirol® ATO 5 (P5), and (E) and (F) for 50:50 w/w ratio blend of the two. Mixtures containing liquid lipid were prepared by substituting 30% w/w of the solid lipid content with Miglyol® 812. The normalised curves were shifted along the ordinate and presented in sets for better visualisation. Arrows are used to pinpoint certain thermal events.

versibility of the thermal events occurring during melting can be detected during re-crystallisation. Overall, tempering or addition of curcumin did not cause any changes to the melting or re-crystallisation characteristics of glyceryl behenate. Addition of Miglyol® 812 resulted in broadening and shifting of the main peak for both thermograms, with a second very broad peak at 55°C appearing in the latter, attributed to a sub-α modification of the monoglyceride fraction of behenic acid (Freitas & Müller, 1999). The difference between the melting and onset temperature (ΔT) represents the range over which the melting event occurs, and therefore a greater difference can be taken as a measure of disorder of the lipid crystals and generation of more amorphous structures (Severino et al., 2011; Souto, Mehnert, & Müller, 2006), which was a feature recorded for the melting thermogram (*Table S3*). However, this observation is contradicted by the melting enthalpy increase. Both thermal events suggest increased crystallinity after the introduction of curcumin in the binary lipid mixture, denoted by the higher enthalpy values and shifting of the exothermic peak to higher temperature. Similar data of increased enthalpy after active addition to the lipid melt have been reported for binary and ternary mixtures of Precirol® ATO 5 and Transcutol® HP with didanosine (DDI) (Kasongo et al., 2011a), and for mixtures of the solid lipid Imwitor® 900 with the poorly water soluble drug RMZE98 (Zimmermann, Souto, & Müller, 2005). Nnamani *et al.* (2014) demonstrated that at a relatively low addition of the water-soluble drug artemether, same to the percentage used in the current study (0.5% w/w), the melting enthalpy was higher than the respective blank binary mixture of Gelucire® 43/01 and Transcutol® P, at a 70:30 w/w ratio.

The DSC thermograms of bulk glyceryl palmitostearate revealed that melting occurs between 56 and 63°C, with a main endothermic peak at 58.2°C bearing a shoulder at 63°C (*Fig. 2C*), while re-crystallisation showed a broad exothermic peak ranging between 42 and 59°C, with one main signal at 58.2°C and two lower intensity signals at 52.4 and 47.4°C (*Fig. 2D*). Tempering caused distinct changes in both profiles, with peak shifting and melting enthalpy reduction. The melting profile recorded in this study shows similarities with the curves obtained for temperatures in the higher spectrum, as reported by Reitz *et al.* (2007), who showed that for glyceryl palmitostearate the obtained profile is tempering temperature-dependent. The main melting peak in the bulk lipid has been attributed to a stable β modification that transforms to a less stable α modification after tempering (peak at 54.8°C), based on wide-angle X-ray scattering (WAXS) measurements (Kasongo et al., 2011b). The decrease in the intensity of the peak at 63°C, could imply that this event occurs due to the presence of components in lower percentages (i.e. triesters). Tempering is a process known to induce changes in the proportion between polymorphs, promoting the formation of the more stable one(s), which could explain the observed temperature and intensity shifting of the peaks (Sato, 2001). As reported earlier, the presence of MCTs can promote the appearance of signals belonging to α polymorphs, in this case at 52.8°C in the melting and at 48.6°C in the cooling thermograms, the intensity of which can vary depending on the type and percentage of liquid lipid used (Cirri et al., 2018; Kasongo et al., 2011a). In contrast to glyceryl behenate, CRM addition led to changes in the melting profile and enthalpy only for the single lipid mixture with glyceryl palmitostearate, while the melting and crystallisation characteristics of binary lipid mixture remained unaffected.

In the melting profile of the glyceryl palmitostearate and glyceryl behenate mixture (*Fig. 2E*), the discrete characteristic glyceride endothermic events can be clearly recognised at 55.5 and 64.0°C, respectively. A small suppression in the glyceryl behenate melting temperature was observed, compared to the thermogram of the singly tempered lipid, possibly caused by the presence of glyceryl palmitostearate. The profile obtained here is somewhat intermediate to the profiles reported by Hamdani *et al.* (2003) that investigated 40:60 and 60:40 w/w ratios of the same solid lipids. Addition of MCTs caused a shift of the melting and crystallisation events to lower temperatures and a ΔT increase (*Table S5*). Even though a level of compatibility between the two solid lipids, due to inter-solubility of their monoacid triglyceride components (Bunjes, Westesen, & Koch, 1996), could be responsible for the identified melting temperature decrease, complete separation of the melting peaks when MCTs was added, indicates that potentially the lipids also co-exist as somewhat separate entities within the blend. The curcumin-loaded binary and ternary lipid mixtures were almost identical to the blank samples, with the exception of the emergence of a small shoulder at 48.8°C at the binary mixture; also identified in the curcumin-loaded glyceryl palmitostearate mixture (*Fig. 2E*). Reversibility of the endothermic events was detected in the re-crystallisation curves for all combinations (*Fig. 2F*). In all cases, the occurrence of distinct re-crystallisation of the two solid lipids is in support of the observations (based on the melting curves) that they co-exist in the blend, while the presence of a miscible blend could only be supported by lowering of the re-crystallisation temperature compared to their individual exothermic events (Kovačević, Müller, & Keck., 2020).

Based on the data acquired from the DSC analysis, the thermal properties of both solid lipids seem to be influenced by the presence of additional components, as reflected by the altered thermal profiles and melting enthalpies. A certain discrepancy to the melting enthalpy trend after the addition of liquid lipid or active between the two solid lipids is recorded. In literature, melting enthalpy reduction has been widely presented in support of incorporation of either the liquid lipid or active within the lipid matrix, and creation of defects in the crystalline structure (Kasongo, & Walker, 2019; Kovačević, Müller, & Keck, 2020; Souto & Müller, 2005; Souto, Mehnert, & Müller, 2006), although it is not always clear whether the reported enthalpy reflects changes to the behaviour of the lipid phase in its entirety, or the crystallising material specifically. For the lipids examined in this study, a common occurrence in all combinations was the increased melting enthalpy values when the liquid lipid was added, as opposed to the active addition, that demonstrated a behaviour reliant on the relative solid-to-liquid lipid combination. The presence of liquid lipid can prompt acceleration of polymorphic transitions to more stable transformations in a concentration-dependent manner (Yoshino, Kobayashi, & Samejima, 1982), that has also been described for dispersed active in the liquid state (Bunjes et al., 2001). Therefore, it could be proposed that the observed thermal profile and enthalpy changes were the result of solubility between the solid and liquid lipids, rather than mixed crystal formation, as has been previously reported for tripalmitin or tristearin binary mixtures with triolein (Norton et al., 1985).

3.3. Characterisation of blank and curcumin-loaded SLNs and NLCs

3.3.1. Particle size, polydispersity and zeta potential

Part of the preliminary lipid dispersion preparation studies was focused on the reduction of the particle size to ensure that the developed systems would be within the desirable size range (sub-micron particles) to act as Pickering emulsion stabilisers (Rousseau, 2000; Zafeiri et al., 2017a). Parameters associated with the processing stage were initially evaluated. More specifically, the duration of the homogenisation step, in this case sonication, was assessed for Precirol® ATO 5 and Compritol® 888 ATO SLNs (5% w/w total lipid content) and using 1.2% w/w PVA as the surfactant. For both lipids, it is quite evident that as the sonication time increases from 1 to 5 minutes (95% amplitude), the average particle size decreases (*Fig. 3A*), which could be explained by the fact that at longer sonication duration greater energy input can be conveyed to the pre-emulsion leading to more efficient droplet breakage, as it has been previously reported (Das et al., 2011b; Kumar et al., 2018). In a next step, formulation parameters were investigated; using both types of solid lipids and at the same lipid concentration, SLNs were fabricated with four types of surfactants at 1.2% w/w (*Fig. 3B*), with Tween® 80 and Pluronic® F-68 generating the smallest particle sizes for both lipids. Subsequently, the lipid concentration was decreased to 2.5% w/w that resulted in a significant particle size reduction (*Fig. 3C*), potentially due to a decrease in the droplet/particle collision events taking place at this

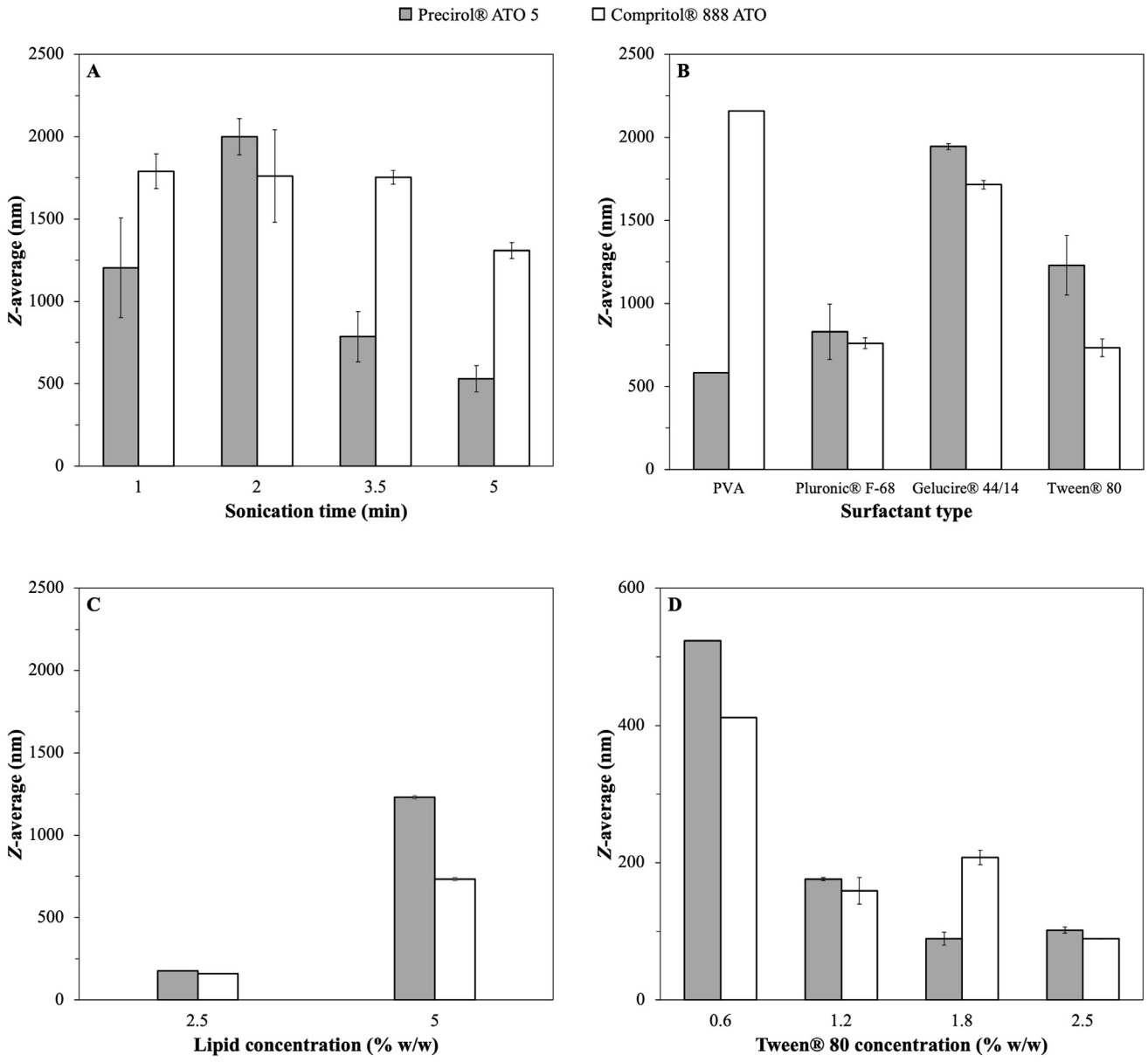

Fig. 3. Particle size of SLNs (*Z*-average) prepared with either Precirol® ATO 5 or Compritol® 888 ATO, when different processing and formulation parameters were used; (A) sonication time, (B) type of surfactant, (C) lipid concentration (% w/w) and (D) concentration of Tween® 80 (% w/w).

lower lipid content (Freitas & Müller, 1999). Lastly, evaluating the effect of the concentration of Tween® 80 using 0.6, 1.2, 1.8 and 2.5% w/w, revealed that increasing the concentration from 0.6 to 1.2% w/w caused a significant decrease in the obtained particle size (*Fig. 3D*). However, further increase in surfactant content had a much smaller effect on the final average particle size, a phenomenon which has been previously described elsewhere (Helgason et al., 2009). The surface active agents have a dual role in the fabrication of lipid particles; provide sufficient interfacial coverage/stabilisation to the droplets during the melt-emulsification stage, while hindering inter-droplet association during the cooling step (crystallisation). The presence of a higher number of surface active molecules in the system can lead to acceleration of interfacial coverage and smaller droplet sizes during the emulsification/droplet breakage step. Although, this event can be counterbalanced by the increased frequency of collisions occurring between droplets of smaller sizes, thus reaching a size reduction plateau at certain surfactant concentration. Hence, the sonication time used was fixed at 5 minutes, the lipid concentration was set at 2.5% w/w, and Tween® 80 and Pluronic® F-68 at 1.2% w/w were the chosen surfactants and concentration for subsequent experiments. Using these optimised formulation/processing parameters, aqueous dispersions of both SLNs and NLCs were prepared according to the compositions presented in *Table 2*. Concerning the formulation characteristics, the type of solid lipid, the concentration of the liquid lipid and the type and concentration of the employed surface active species were all explored, in terms of their effect on the size of the formed SLN and NLC particles.

Initially, lipid particle dispersions were prepared with Compritol® 888 ATO in the absence of curcumin by progressively replacing 10, 20 and 30% w/w of the solid lipid mass with Miglyol® 812 (formulations B-SLN$_1$ and B-NLC$_1$–B-NLC$_3$). All formulations displayed monomodal size distributions, with sizes ranging between 140 and 160 nm. It was observed that addition of the liquid lipid did not result in particle size or distribution profile changes for 10% w/w, and it was only at 20% w/w that a statistically significant ($p<0.05$) decrease was recorded (*Fig. 4A* & *Table 3*). At 30% w/w liquid lipid, a plateau in terms of size was reached, with no further particle size variations. Correspondingly, the

Table 2
Composition of SLN and NLC formulations prepared with Precirol® ATO5, Compritol® 888 ATO or 1:1 w/w ratio of the two as solid lipid matrix, Miglyol® 812 as the liquid lipid at various concentrations (10, 20 and 30% w/w of the lipid phase), and Tween® 80 or Pluronic® F-68 as surfactants, either blank or loaded with curcumin.

Formulation	Compound concentration (% w/w)						
	Compritol® 888 ATO	Precirol® ATO 5	Miglyol® 812	Tween® 80	Pluronic® F-68	Curcumin	Water
B-SLN_1	2.5	-	-	1.2	-	-	96.3
B-NLC_1	2.25	-	0.25	1.2	-	-	96.3
B-NLC_2	2.0	-	0.5	1.2	-	-	96.3
B-NLC_3	1.75	-	0.75	1.2	-	-	96.3
SLN_1	2.4875	-	-	1.2	-	0.0125	96.3
NLC_1	2.2388	-	0.2487	1.2	-	0.0125	96.3
NLC_2	1.99	-	0.4975	1.2	-	0.0125	96.3
NLC_3	1.7413	-	0.7462	1.2	-	0.0125	96.3
SLN_2	-	2.4875	-	1.2	-	0.0125	96.3
NLC_4	-	1.7413	0.7462	1.2	-	0.0125	96.3
SLN_3	1.2438	1.2437	-	1.2	-	0.0125	96.3
NLC_5	0.8707	0.8707	0.7461	1.2	-	0.0125	96.3
SLN_4	2.4875	-	-	0.5	-	0.0125	97
SLN_5	2.4875	-	-	-	1.2	0.0125	96.3

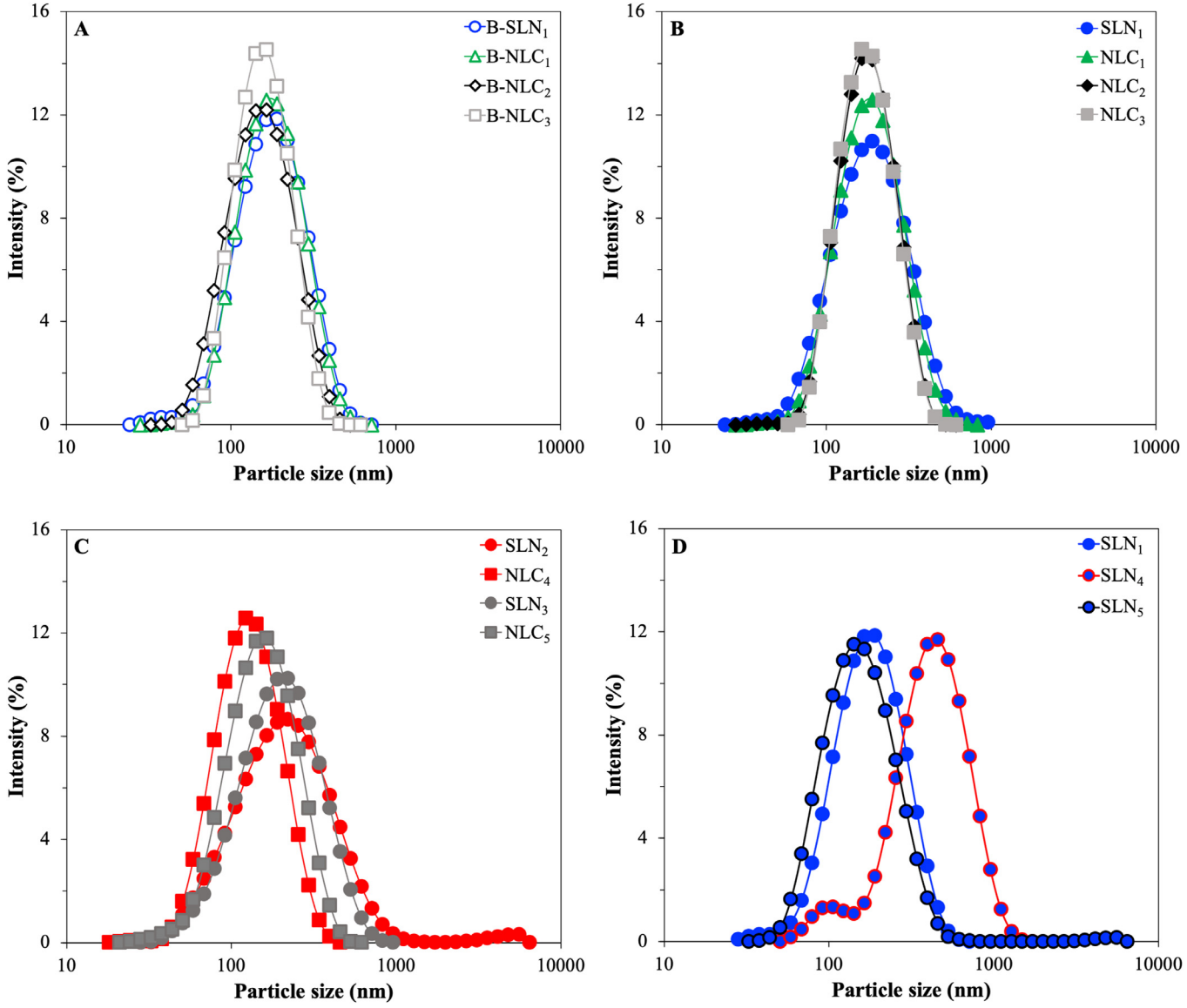

Fig. 4. Dynamic light scattering measurements showing the particle size distribution of SLN and NLC formulations after preparation. (A) Formulations B-SLN_1 and B-NLC_1–B-NLC_3, (B) SLN_1 and NLC_1–NLC_3, (C) SLN_2–SLN_3 and NLC_4–NLC_5, and (D) SLN_1 and SLN_4–SLN_5.

Table 3
Z-average, polydispersity index (PDI) and zeta potential (ζ-potential) of different SLN and NLC formulations measured after preparation.

Formulation	*Z*-average (nm)	PDI	ζ-potential (mV)
B-SLN$_1$	158.9 ± 10.6	0.20 ± 0.02	-23.0 ± 1.3
B-NLC$_1$	160.5 ± 3.8	0.16 ± 0.02	-22.3 ± 1.9
B-NLC$_2$	140.4 ± 20.1	0.15 ± 0.02	-19.5 ± 2.6
B-NLC$_3$	145.8 ± 3.4	0.12 ± 0.02	-20.1 ± 0.7
SLN$_1$	165.1 ± 2.7	0.20 ± 0.02	-25.2 ± 2.6
NLC$_1$	165.4 ± 5.3	0.16 ± 0.02	-25.0 ± 3.0
NLC$_2$	162.5 ± 6.5	0.13 ± 0.01	-21.7 ± 1.3
NLC$_3$	163.2 ± 3.8	0.12 ± 0.01	-20.5 ± 0.7
SLN$_2$	176.0 ± 9.6	0.28 ± 0.04	-32.7 ± 0.9
NLC$_4$	114.4 ± 7.1	0.14 ± 0.04	-26.0 ± 2.7
SLN$_3$	170.9 ± 15.2	0.23 ± 0.01	-27.6 ± 1.4
NLC$_5$	136.2 ± 2.5	0.19 ± 0.01	-24.4 ± 1.9
SLN$_4$	343.9 ± 26.5	0.24 ± 0.03	-29.0 ± 2.8
SLN$_5$	139.7 ± 1.9	0.20 ± 0.01	-24.4 ± 0.7

PDI showed a distinctive trend of decreasing values for NLCs of increasing liquid lipid content. Incremental incorporation of MCTs (up to 20% w/w) causing changes in the viscosity of the glyceryl behenate melt droplets could be responsible for the gradual decrease in the particle size and PDI of the lipid particles obtained after crystallisation. Gokce *et al.* (2012) reported that the incorporation of different percentages of MCTs in the solid matrix of glyceryl behenate overall resulted in reduced particle sizes of the NLCs compared to the respective SLNs, which was attributed to more effective homogenisation and improved energy transfer due to the liquid lipid presence. Similarly, in another study, Hu *et al.* (2005) reported that incorporation of 30% w/w of the liquid lipid oleic acid in stearic acid reduced both the viscosity and surface tension in the lipid melt droplets, thus ultimately resulting in the formation of smaller NLC particles (164.6 nm compared to the 379.7 nm in the formulation without any oleic acid). Incorporation of curcumin to the blank lipid dispersions led to a slight increase in the particle sizes for all systems (SLN$_1$ and NLC$_1$–NLC$_3$), which amongst them however displayed almost identical sizes, irrespective of the solid-to-liquid lipid mass ratio. Comparison between the blank and curcumin-loaded dispersions, showed a significant size increase only for the 20 and 30% w/w NLC formulations (NLC$_2$, NLC$_3$). This behaviour has been reported previously, when the average sizes of blank and active-loaded SLNs and NLCs were compared, and was attributed to a combination of swelling of the lipid core due to active encapsulation and increase of the interfacial tension and/or viscosity of the dispersed phase causing inefficient particle size reduction (Akhoond Zardini et al., 2018; Hu et al., 2005; Tamjidi et al., 2014). Both the size distribution profiles (*Fig. 4B*) and PDI values for the CRM-loaded SLNs/NLCs systems remained unaffected.

The size characteristics of the particles produced using Precirol® ATO 5 as the solid lipid were also evaluated. Glyceryl palmitostearate SLNs (SLN$_2$) displayed a slightly broader size distribution (higher PDI value) and larger particle sizes in comparison to SLNs composed of glyceryl behenate (SLN$_1$). These findings, possibly outline the impact of the processing parameters, and more specifically the duration of the sonication step. The statistically significant increase to the *Z*-average due to the presence of an additional small peak identified at 5.5 μm in SLN$_2$ could have been caused by excess energy transfer to the system inducing extreme acoustic cavitation and temperature rise (starting at 70°C prior to sonication to 94°C after sonication), resulting in enhanced pre-emulsion droplet breakage and coalescence (*Fig. 4C*) (Canselier et al., 2001; Kentish et al., 2008). Inversely, comparing formulations NLC$_3$ and NLC$_4$ (NLCs fabricated with glyceryl behenate and glyceryl palmitostearate, respectively), reveals that the latter were characterised by smaller *Z*-average values. The overall lower viscosity of the Precirol® ATO 5/Miglyol® 812 blend to the equivalent Compritol® 888 ATO NLCs could explain the lower particle sizes. The combination of the characteristics of the two solid lipids can be accounted for the somewhat intermediate behaviour that was observed for both the SLN and NLC formulations fabricated with 1:1 mass ratio mixture of the two (SLN$_3$–NLC$_5$).

In regard to the particles formed with different surfactant parameters, Compritol® 888 ATO SLNs were produced using 1.2% and 0.5% w/w Tween® 80 (SLN$_1$ and SLN$_4$, respectively), and 1.2% w/w Pluronic® F-68 (SLN$_5$) (*Fig. 4D*). Particles prepared with reduced surface active species concentration (SLN$_4$) (to study the relation between surfactant concentration/particle size with curcumin loading in a next step), showed bimodal size distribution profile, with higher *Z*-average and PDI compared to the respective formulation of higher surfactant concentration (SLN$_1$). The lack of sufficient number of surface active species to fully cover and stabilise the pre-emulsion droplets creates a system that is more prone to coalescence, particularly under relatively high sonication durations (5 min), when the chances of droplet collisions are increased due to the combination of high energy input and long period of interaction. In contrast, Pluronic® F-68 (Poloxamer 188) appeared to drive the SLN size reduction a bit further than Tween® 80 (SLN$_1$), implying better coalescence hindrance, leading to smaller lipid particles after crystallisation. The effect of the characteristics and concentration of surfactant on the resultant particle size has been previously highlighted in a study by Zafeiri *et al.* (2017a).

In terms of the zeta potential values acquired, all glyceryl behenate-containing lipid dispersions were characterised by values ranging between 19 and 25 mV (*Table 3*), without any major changes identified after the addition of curcumin. A slight decrease with increasing liquid lipid concentration for both blank and curcumin-loaded lipid dispersions, but also for all types of solid lipid compositions can be seen, suggesting a reduction to the particles' surface potential and further indicating changes at the surface of the NLCs; such as potential shifts in the shear plane (Fang et al., 2008; Kovacevic et al., 2011; Makoni, Kasongo, & Walker, 2019; Müller, Mäder, & Gohla, 2000). SLNs prepared with Tween® 80 did not differ significantly from lipid dispersions fabricated with Poloxamer 188 in their zeta potential values (formulations SLN$_1$ and SLN$_5$, respectively), while the formulation with lower concentration of the former (Tween® 80) yielded particles with higher ζ-potential (SLN$_4$). The negative charge in all formulations is attributed to the presence of free fatty acids at the surface of the particles, as both types of surfactants are non-ionic (Kovacevic et al., 2011).

3.3.2. Thermal analysis of aqueous lipid dispersions

DSC analysis was used to gain a better insight on the effect of the specific particle characteristics and varying formulation parameters on the thermal properties and crystallinity of the produced SLNs and NLCs (shown in *Table 2*). These are important factors when it comes to predicting the long-term physical stability of the lipid nanoparticles, but also their ability to maintain physical integrity both in terms of active expulsion phenomena and liquid lipid expulsion/separation (in the case of NLCs) (Freitas & Müller, 1999; Kovacevic et al., 2011; Westesen, Bunjes, & Koch, 1997). The melting and crystallisation thermograms are presented in *Fig.s 5 and 6*, respectively.

Comparison between the lipid nanoparticles prepared with glyceryl behenate and combination with MCTs at 70:30 w/w ratio (systems B-SLN$_1$ and B-NLC$_3$), and their respective physical mixtures reveals peak broadening and shifting towards lower temperatures (*Fig.s 5A & B*). According to the Gibbs-Thompson effect, sub-micron sized solid lipid particles can reach thermodynamic equilibrium at lower temperatures compared to the larger crystals in their (pure lipid) physical mixtures (Jenning, Thünemann, & Gohla, 2000b; Kovacevic et al., 2011; Perez, 2005). In addition, polymorphic transitions and crystallisation process modulation can be further prompted by the adsorption of surfactant molecules on the lipid particle surface, explaining changes in the melting and crystallisation profiles (Bunjes, Koch, & Westesen, 2002). A level of polymorphism can be identified in the SLN formulation, due to the presence of a split (at 68.9°C) on the main peak (70.7°C), that

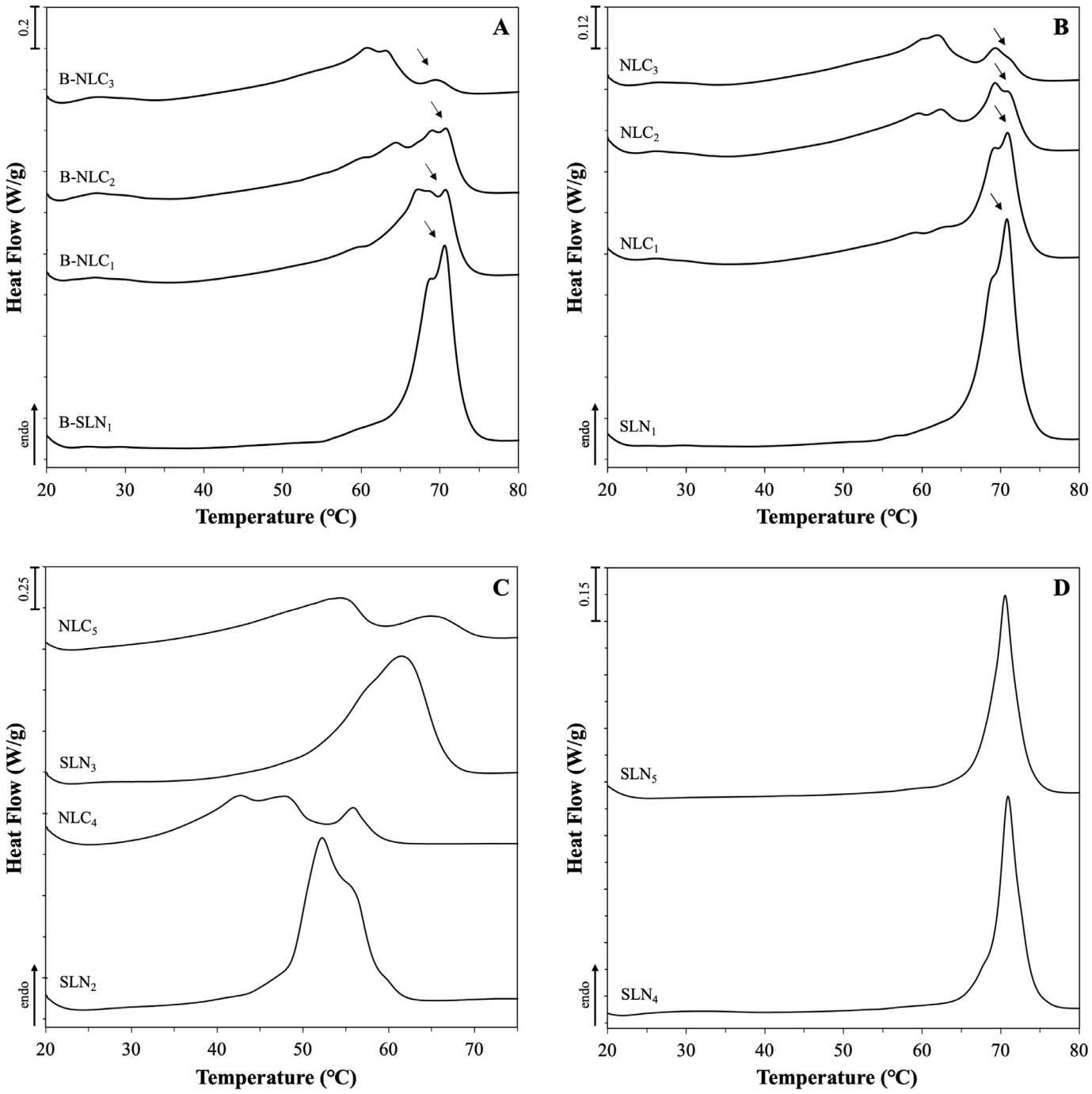

Fig. 5. DSC melting curves of SLN and NLC aqueous dispersions consisting of Miglyol® 812 as the liquid lipid in combination with different solid lipids or blends of them. Graphs (A), (B) and (D) show the melting behaviour of formulations prepared with Compritol® 888 ATO without curcumin, with 0.0125% w/w curcumin and with varying type or concentration of surfactants, respectively. Graph (C) displays the melting curves of formulations fabricated with either Precirol® ATO 5 or blend of the two solid lipids at 50:50 w/w ratio. The exact composition of the formulations can be found in Table 2. The normalised curves were shifted along the ordinate and presented in sets for better visualisation. Arrows are used to pinpoint certain thermal events.

has also been shown in the data reported by Jenning *et al.* (2000) and Freitas *et al.* (1999), albeit the split appeared at higher temperatures (approximately at 75 and 73°C, respectively). This discrepancy could be attributed to the varying surfactant to lipid ratio, with the proportion used in this study being higher (approximately 1:2) than the almost 1:8 used in the aforementioned studies, or differences in the fabrication/analysis conditions. As discussed earlier, Compritol® ATO 888 is a composite mixture of behenic acid esters, which could account for the complex polymorphic behaviour of the resulting lipid particle dispersions, particularly so in the presence of MCTs. In the work by Jenning *et al.* (2000), both SLNs and NLCs with various solid-to-liquid lipid mass ratios exhibited the metastable β', while increasing amount of intermediate β_i polymorphs were also identified in the NLCs with increasing MCTs concentration, as suggested by wide-angle X-ray scattering (WAXS) measurements. Pronounced polymorphic transitions in the presence of MCTs were additionally suggested by the recrystallisation thermograms of the SLNs displaying a main thermal event bearing a shoulder peak at a lower temperature, that became progressively more intense with increasing

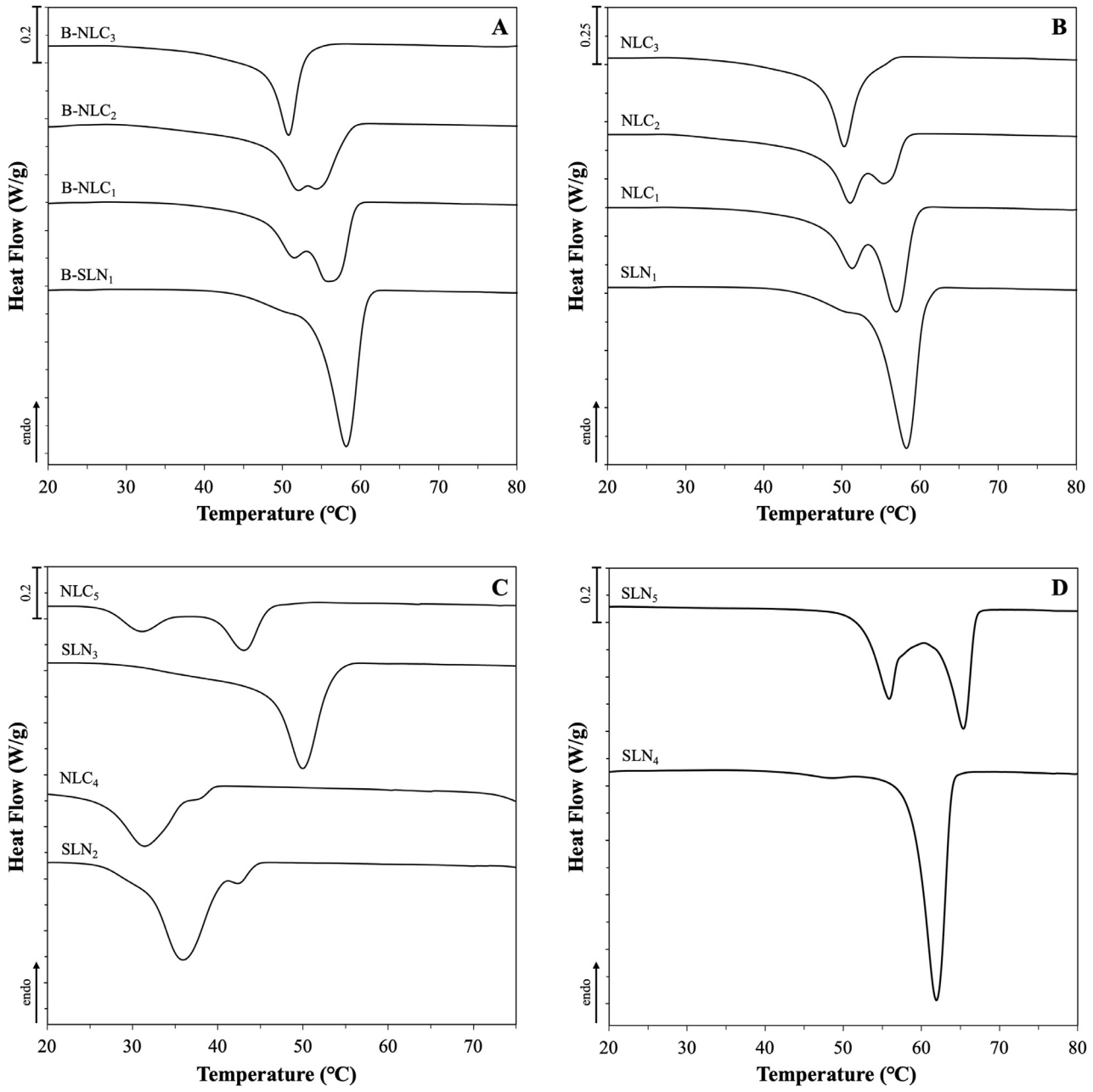

Fig. 6. DSC crystallisation curves of SLN and NLC aqueous dispersions consisting of Miglyol® 812 as the liquid lipid in combination with different solid lipids or blends of them. Graphs (A), (B) and (D) show the melting behaviour of formulations prepared with Compritol® 888 ATO without curcumin, with 0.0125% w/w curcumin and with varying type or concentration of surfactants, respectively. Graph (C) displays the crystallisation curves of formulations fabricated with either Precirol® ATO 5 or blend of the two solid lipids at 50:50 w/w ratio. The exact composition of the formulations can be found in Table 2. The normalised curves were shifted along the ordinate and presented in sets for better visualisation.

liquid lipid concentration, ultimately being the main peak for the B-NLC_3 and NLC_3 formulations (*Fig.s 6A & B*). Addition of the active in formulations B-SLN_1 and B-NLC_1–B-NLC_3 appears to have somewhat altered the polymorph ratios, as implied by the differences in the relative peak intensities in both the melting and re-crystallisation thermograms (*Fig.s 5B & 6B*).

Variations in the thermal event characteristics could provide further information regarding the impact imposed by the oil (liquid lipid) and/or active incorporation to glyceryl behenate, which is the only component undergoing phase transition within the particle structure. As the liquid lipid concentration increases in both blank and curcumin-loaded lipid particles, the melting and onset temperatures display a negative slope, with the width of melting significantly increasing from the SLNs to the NLCs with 20% w/w liquid lipid (*Table 4* & *Fig. 7A*). Accordingly, looking at the melting enthalpy trend, gradual increase of MCTs in formulations B-NLC_1-B-NLC_3 shows that at 20% w/w mass and beyond, there was a pronounced reduction in the melting enthalpy of the crystalline matter compared to formulation B-SLN_1 (*Table 4* & *Fig. 7B*). Lipid phase crystallinity loss was suggested by the recrystallisation indices (RI), which showed a linear decreasing trend with increasing MCTs concentration. RI values of over 100% could be attributed to the presence of a more stable polymorph in the lipid particles compared to the bulk lipid, in this case the β_i form distinguishable in all formulations (peaks indicated by arrows in *Fig.s 5A & B*); a transformation that has been previously described for glyceryl behenate particles kept in storage (Jenning, Schäfer-Korting, & Gohla, 2000a). A distinction between the

Table 4
DSC melting and crystallisation parameters of SLN and NLC aqueous dispersions. Enthalpy values (ΔH) reflect the total enthalpy measured after integration of all thermal events present. The maximum melting and crystallisation (T_{max}) and onset (T_{onset}) temperatures are given for the individual occurring thermal events, as well as the width between the two (ΔT) and the recrystallisation index (RI) for each formulation.

		ΔH (J/g)	T_{max} (°C)	T_{onset} (°C)	ΔT (°C)	RI (%)
B-SLN$_1$	**Melting**	140.1 ± 3.2	70.7 ± 0.2	65.6 ± 0.2	5.1 ± 0.4	106.8 ± 3.2
	Crystallisation	-149.4 ± 2.2	58.2 ± 0.3	60.6 ± 0.3	-2.4 ± 0.2	
B-NLC$_1$	**Melting**	141.3 ± 14.4	68.9 ± 2.7	62.4 ± 1.5	6.5 ± 1.3	97.0 ± 9.9
	Crystallisation	-120.6 ± 25.7	55.9 ± 1.0	59.1 ± 0.8	-3.2 ± 0.2	
B-NLC$_2$	**Melting**	115.1 ± 2.9	64.0 ± 0.3	50.9 ± 1.8	13.1 ± 1.1	79.0 ± 2.0
	Crystallisation	-114.8 ± 2.6	51.5 ± 0.1	56.9 ± 1.8	-5.4 ± 1.7	
B-NLC$_3$	**Melting**	98.6 ± 3.4	60.7 ± 0.1	44.7 ± 0.3	16.0 ± 0.3	67.7 ± 2.3
	Crystallisation	-97.0 ± 3.3	50.8 ± 0.1	53.2 ± 0.6	-2.4 ± 0.7	
SLN$_1$	**Melting**	146.8 ± 2.2	70.8 ± 0.1	65.4 ± 0.8	5.4 ± 0.8	101.9 ± 1.8
	Crystallisation	-148.8 ± 1.6	58.3 ± 0.1	60.7 ± 0.2	-2.4 ± 0.1	
NLC$_1$	**Melting**	147.7 ± 3.5	70.8 ± 0.1	62.4 ± 0.3	8.3 ± 0.3	101.4 ± 2.4
	Crystallisation	-146.7 ± 4.2	57.0 ± 0.2	59.4 ± 0.1	-2.5 ± 0.2	
NLC$_2$	**Melting**	148.7 ± 11.3	69.3 ± 0.1	47.4 ± 0.5	21.9 ± 0.5	90.6 ± 6.7
	Crystallisation	-138.3 ± 4.8	51.1 ± 0.1	58.2 ± 0.1	-7.1 ± 0.1	
NLC$_3$	**Melting**	139.1 ± 7.1	61.9 ± 0.1	46.5 ± 0.2	15.5 ± 0.2	74.2 ± 3.8
	Crystallisation	-130.6 ± 5.5	50.3 ± 0.2	53.4 ± 0.2	-3.1 ± 0.3	
SLN$_2$	**Melting**	157.4 ± 5.2	52.3 ± 0.1	47.7 ± 0.1	4.5 ± 0.1	89.1 ± 2.9
	Crystallisation	-138.6 ± 3.5	36.0 ± 0.3	41.8 ± 1.1	-5.9 ± 1.2	
NLC$_4$	**Melting**	144.6 ± 8.8	46.3 ± 3.4	35.2 ± 0.3	11.1 ± 3.2	57.3 ± 3.5
	Crystallisation	-121.0 ± 3.6	31.4 ± 0.3	36.4 ± 0.1	-5.0 ± 0.4	
SLN$_3$	**Melting**	162.3 ± 21.0	61.5 ± 0.6	49.5 ± 1.3	11.9 ± 1.0	104.0 ± 9.7
	Crystallisation	-140.1 ± 22.3	48.9 ± 0.5	53.2 ± 0.2	-3.4 ± 0.2	
NLC$_5$	**Melting**	142.2 ± 6.6	53.7 ± 0.7	36.0 ± 0.6	17.7 ± 0.2	64.7 ± 3.0
	Crystallisation	-114.5 ± 2.4	43.1 ± 0.2	46.0 ± 0.3	-2.8 ± 0.5	
SLN$_4$	**Melting**	152.2 ± 3.9	71.3 ± 0.1	69.0 ± 0.3	2.3 ± 0.3	115.3 ± 3.0
	Crystallisation	-154.2 ± 6.2	61.9 ± 0.1	63.9 ± 0.1	-2.0 ± 0.1	
SLN$_5$	**Melting**	156.0 ± 7.2	71.0 ± 0.0	68.6 ± 0.1	2.4 ± 0.1	116.9 ± 5.5
	Crystallisation	-156.6 ± 7.9	65.4 ± 0.1	66.9 ± 0.1	-1.5 ± 0.0	

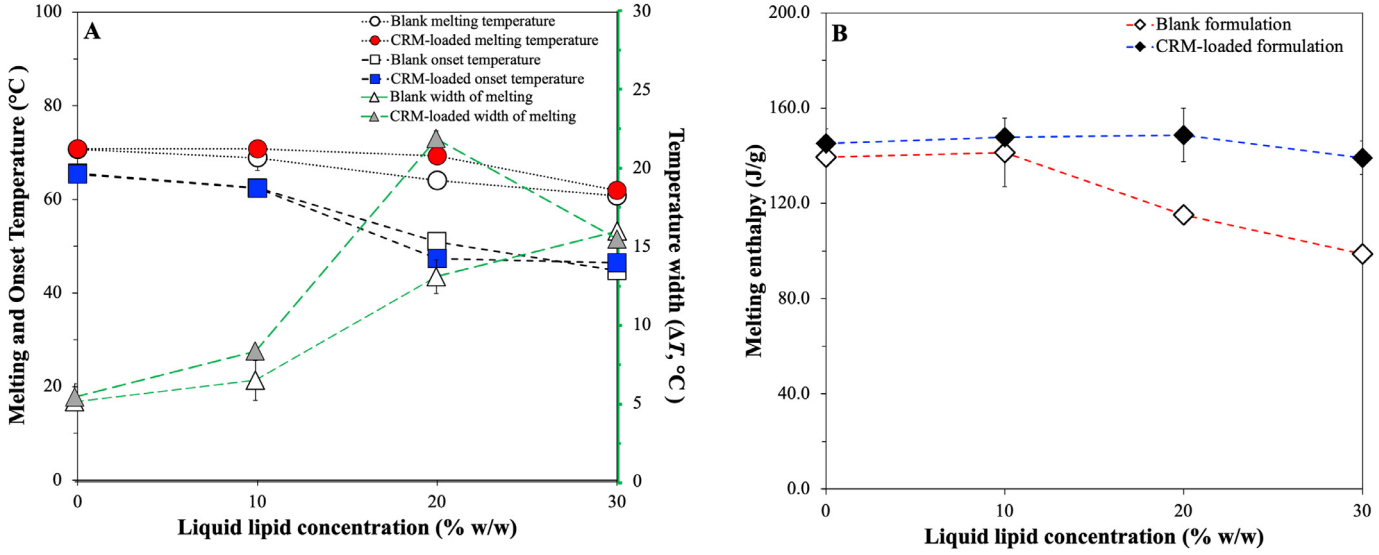

Fig. 7. (A) Melting and onset temperature, and width between these two temperatures trends, and (B) melting enthalpy trends at increasing liquid lipid concentration from 0% to 30% w/w for blank (B-SLN$_1$ and B-NLC$_1$–B-NLC$_3$) and CRM-loaded formulations (SLN$_1$ and NLC$_1$–NLC$_3$).

information extracted from these two parameters needs to be made at this point; RI value comparison reflects changes to the lipid phase, as the total mass of the lipid phase used for calculations is not accounting for solid lipid mass reductions in NLCs, while enthalpy data signify variations in the crystallising matter behaviour. Bunjes *et al.* (2007) attributed the melting point depression of glyceryl behenate/medium chain triglycerides nanoparticles on eutectic behaviour, although a slight solubility between the components was not excluded. Combining the ΔH and RI trends with the findings from the physical mixtures indicating partial solubility between the two lipids, a liquid lipid incorporation in the lattice created by the solid lipid, leading to a less ordered internal crystalline structure could be proposed. However, the pattern of non-linear relationship between the interval increase of MCTs and the thermal properties does not allow excluding the occurrence of oil phase separation within the lipid particles at higher liquid lipid concentrations. This is in accordance with previously reported data in literature indicating a liquid lipid concentration-dependent formation of distinct lipid structures (Jenning, Thünemann & Gohla, 2000b; Jores, Mehnert, & Mäder, 2003). An equivalent behaviour of the melting enthalpy was not however inherited to the formulations containing curcumin (SLN$_1$

and NLC_1–NLC_3), for which no statistically significant deviations were recorded. Comparison of the ΔH and RI values between blank and CRM-loaded formulations demonstrated, that systems NLC_2 and NLC_3 were characterised by a statistically significant crystallinity increase. These observations for both blank and CRM-loaded formulations are consistent with the particle size trends reported earlier (*Section 3.3.1*). Incorporation of curcumin in the particles conveys an effect on their thermal behaviour that appears to be reliant on the relative solid-to-liquid lipid ratio, and possibly on the extent to which the liquid lipid addition affects the physical properties of the crystalline lipid matrix, as demonstrated by both melting and crystallisation temperature, and enthalpy characteristics.

Following the investigations using glyceryl behenate, curcumin-loaded SLNs and NLCs with 30% w/w liquid lipid content were fabricated with glyceryl palmitostearate. As expected, Precirol® ATO 5 SLNs (SLN_2) and NLCs (NLC_4) demonstrated lower melting and crystallisation maxima as opposed to the respective CRM-containing physical mixtures (*Fig.s 5C & 6C*). Incorporation of MCTs in the pre-emulsion blend (NLC_4) enhanced the polymorphism, and led to reduction of the ΔH and melting temperature, and increase in the RI and ΔT values. Possible explanations could lie on the creation of a less crystalline lipid matrix after incorporation of the liquid lipid, statistically significant particle size reduction compared to the SLNs, or combination of the two. The relative behaviour between formulations SLN_2 and NLC_4 is similar to the corresponding glyceryl behenate formulations (SLN_1 and NLC_3), albeit the decrease of the melting width of the former was lower comparatively. This is likely underlining the impact of the surfactant on the overall thermal behaviour of the particles, which appears to have been greater in the case of the glyceryl behenate formulations compared to glyceryl palmitostearate. Indeed, Fang *et al.* (2008) did not detect any melting point shifts caused by the addition of Tween® 80 in the physical mixtures of glyceryl palmitostearate and squalene. The effect of the type and chemistry of the surfactant not only on the resulting particles size, but also on the interactions developed with the crystalline matrix depending on its composition has been previously shown to be important parameters governing the particles' crystalline properties (Zafeiri et al., 2017a).

The co-existence of the individual solid lipids within a partially miscible blend of them, which was hypothesised based on the DSC data of their physical mixtures, cannot be ruled out also for their SLNs (SLN_3) and NLCs (NLC_5), based on the somewhat intermediate melting behaviour to their singly SLN dispersions, and the peak separation observed in the melting and re-crystallisation profile, respectively (*Fig.s 5C & 6C*). The high RI of formulation SLN_3 (104.0%), which is comparable to that of SLN_1, suggests the presence of high ratio of β_i forms attributed to glyceryl behenate, whereas the intermediate RI of NLC_5 to both NLCs composed of the individual components (NLC_3 and NLC_4) could be the result of the combined accelerated polymorphic transitions of both solid lipids due to the liquid lipid addition. Regarding the thermal profiles of the SLNs with lower surfactant concentration (SLN_4), melting and crystallisation events of reduced 'complexity' can be observed, that could be due to the different packing of the surfactant at the particles' interface as a function of its concentration, compared to formulation SLN_1 (Helgason et al., 2009). On the contrary, the crystallisation profile for the Poloxamer 188 particles appears to be more complex, but in line with data reported in literature (Zur Mühlen, Schwarz, & Mehnert, 1998) for the same combination of solid lipid and surfactant (*Fig. 6D*). In the melting profile of SLN_5 (*Fig. 5D*), the single endothermic peak at 71.0°C that could be attributed to a stable β_i polymorphic form and the higher RI value compared to formulation SLN_1 indicate the existence of a more highly ordered internal lattice. Thus, higher compatibility between glyceryl behenate and Tween® 80 can be postulated, as that would allow part of the surfactant's structure to participate in the crystalline network close to the surface region of the particles, and in a higher degree than Poloxamer 188 molecules, leading to decreased packing of the crystalline structure and transition to less stable polymorphs (β'), observed for Tween® 80 particles.

3.3.3. Encapsulation efficiency and loading capacity

To establish the amount of curcumin incorporated within the lipid particles and evaluate whether the chosen materials were able to achieve high active loadings, the encapsulation efficiency (EE) and loading capacity (LC) were determined. All formulations were characterised by EE and LC values of 99.9 ± 0.0% and 5.0 ± 0.0%, respectively. It appears that changes in the chemical and physical characteristics of the SLN/NLC particles, did not convey any changes to their ability to enclose curcumin. Even when the value of the *Z*-average almost doubled (SLN_4), or the RI was high (SLN_1, NLC_1, SLN_2, SLN_3, SLN_4 and SLN_5), characteristics that are generally considered to have a negative impact on active entrapment (Jia et al., 2010; Souto et al., 2004a), the EE and LC values remained equally high. This is in agreement with other studies using the same materials and similar concentration of the active in relation to the lipid phase. Araujo *et al.* (2020) have recently demonstrated how the composition of NLCs influences curcumin loading, reporting that NLCs prepared with Compritol® 888 ATO and MCT at 0.75% w/w curcumin in the lipid phase had an EE of 88.34 ± 2.84% and LC of 2.22 ± 0.01%. In another study, NLCs prepared with either Compritol® 888 ATO or Precirol® ATO 5 as the solid lipids and Labrasol® as the liquid lipid showed EE ranging between 79.70 and 96.89% and LC between 2.63 and 3.26% for the 0.5% w/w curcumin to lipids concentration used; both EE and LC were found to depend on the type of surfactant used (Tween® 80 or Poloxamer 407) and with higher values attributed to Precirol® ATO 5 (Espinosa-Olivares et al., 2020). In both studies, the method followed for the preparation of curcumin-loaded lipid dispersions involved the simple solubilisation of curcumin in the lipid melts under stirring. The use of solvents, such as ethanol or chloroform, to increase the amount of solubilised curcumin in the lipid phase have been reported to give LC up to 23.38% and EE up to 54% w/w of curcumin in lipid content (Bondì et al., 2017; Wang et al., 2018). In an aforementioned work (Doktorovova, Souto, & Silva, 2017), that explored the selection of a suitable solid lipid for curcumin encapsulation, the authors attempted to increase the percentage of curcumin to 2 and 3% w/w, from the initial 1% w/w that was defined as the maximum soluble quantity, which led to precipitation. Therefore, it is not clear at this stage and following the described processing and formulation parameters, whether increasing the percentage of curcumin in regard to the lipid phase concentration would result in equally high EE and LC values. Since the solubility of the active in the lipid phase changes during crystallisation, maintaining the concentration of the active close to the solubility threshold defined during preliminary solubility studies could explain the high EE and LC achieved in this study.

3.3.4. Storage stability

Formulations fabricated with glyceryl behenate, both blank (B-SLN_1 and B-NLC_1–B-NLC_3) and curcumin-loaded (SLN_1 and NLC_1–NLC_3), showed good storage stability over the examined time, with no deviation in the particle size (*Table S6*), well-maintained thermal profiles (*Table S7*), and unchanged EE and LC values. On the contrary, formulations comprising of glyceryl palmitostearate (SLN_2–SLN_3 and NLC_4–NLC_5) did not preserve their size characteristics above the 4 weeks mark. Physical modifications taking place during ageing of Precirol® ATO 5 have been reported to cause destabilisation of their physical properties to a greater extent than in longer fatty acid chain lipids, such as Compritol® 888 ATO (Hamdani, Moës & Amighi, 2003; Sutananta, Craig, & Newton, 1994). Additionally, the greater temperature difference between the melting and crystallisation temperatures of glyceryl palmitostearate (compared to glyceryl behenate), would mean that droplets maintain their molten state over a longer period (prior to crystallisation) and thus are potentially exposed to a high risk of emulsion instabilities (e.g. coalescence), which in turn ultimately result in the formation of larger particles post-crystallisation (peak at 5.5 μm). The ageing modifications

and/or destabilisation caused by liquid lipid expulsion could be assigned to the oily film formation observed for formulation NLC_4 at four weeks of storage. Since no such observation was made for glyceryl behenate and MCTs formulation, the lower affinity of MCTs for glyceryl palmitostearate that was suggested by the theoretical lipid screening studies could be responsible for this outcome. For samples containing both solid lipids, it was proposed by Bose *et al.* (2013) that the varying rates of crystallisation of the two lipids (period of several months of glyceryl behenate and rapid for glyceryl palmitostearate) resulted in overall faster lipid transformation, leaving limited number of surfactant molecules to cover new surfaces formed during storage-induced lipid transformations, consequently causing aggregation. Changes in the ζ-potential values recorded for most formulations over time can be used as indicators of electrostatic properties variations (Riddick, 1968; Souto et al., 2004b), which in turn is a sign of destabilisation. However, Tween® 80 and Poloxamer 188 are known to provide stabilisation through superposition of electrostatic and steric factors acting synergistically, which explains the stability preservation despite the values lower than $|30|$ mV and their variations (Freitas & Müller, 1998; Tan et al., 2016). Long-term aggregation of Poloxamer 188-stabilised SLNs (SLN_5) confirmed by LD measurements (data not shown) could be the result of electrostatic repulsion losses induced by the bridging effects or gelling properties of block co-polymers like Poloxamer 188, as discussed by Freitas *et al.* (1998). In addition, the pre-existence of larger particles, in this case, as shown in *Fig. 4D* could have further promoted this effect. In instances where insufficient number of surfactant molecules are present in the system (SLN_4), the lipid particle surfaces remain uncovered, allowing for lipid particles to approach each other and result in aggregation, due to the absence of either steric or electrostatic repulsion forces, which was supported by LD data.

4. Conclusions

The present work explores the impact of different formulation parameters on the physical properties of SLNs and NLCs used as carriers of a model hydrophobic active. Theoretical active-to-lipid miscibility predictions, employing the Hansen solubility parameter, aligned well with experimental data, and this lipid screening approach is demonstrated to be an effective tool for selecting lipid components that can achieve high solubilisation of a chosen active; in this case curcumin. Lipid nanoparticles, of dimensions compatible to those required for Pickering functionality, were fabricated with varying combinations of the selected lipid materials and exhibited equally high encapsulation efficiency and loading capacity values, irrespective of their exact composition. Incremental addition of liquid lipid was shown to have a concentration-dependent effect on both the obtained size and thermal behaviour of the formed particles with glyceryl behenate as the solid lipid, while the impact of active incorporation in the same particles was reliant on the relative solid-to-liquid lipid mass ratio. The influence of the compatibility between the lipid matrix components on the size and polymorphism was highlighted. Specifically, this was denoted by investigating the compatibility between solid lipid(s) and liquid lipid, when solid lipids with varying melting and crystallisation temperatures were used, and the affinity of the surfactant to the lipid blend, when different type of surface active species were employed. The formulation approach adopted in this study, whereby pre-formulation compatibility evaluation is performed between the active under investigation and the lipid components, could lead to the generation of a range of diverse lipid structures in terms of their crystalline properties, that are ensured to retain high active loadings over prolonged periods. Future work using the developed systems will aim to investigate/confirm the ability of the lipid particles to act as Pickering emulsion stabilisers, while maintaining their stability and active-carrier functionalities. Additionally, the improved understanding on their crystalline structure properties could be utilised to design/achieve controlled and tailor-made release patterns.

Declaration of Competing interests

The authors declare that they have no known competing financial interests or personal relationships that could have appeared to influence the work reported in this paper.

Acknowledgements

This work was supported by funding from the Biotechnology and Biological Sciences Research Council (BBSRC) through the Midlands Integrative Bioscience Doctoral Training Partnership (BB/M01116X/1).

Supplementary materials

Supplementary material associated with this article can be found, in the online version, at doi:10.1016/j.fhfh.2021.100024.

References

Akhoond Zardini, A., Mohebbi, M., Farhoosh, R., & Bolurian, S (2018). Production and characterization of nanostructured lipid carriers and solid lipid nanoparticles containing lycopene for food fortification. *Journal of Food Science and Technology, 55*(1), 287–298. 10.1007/s13197-017-2937-5.

Anand, P., Kunnumakkara, A. B., Newman, R. A., & Aggarwal, B. B. (2007). Bioavailability of curcumin: Problems and promises. *Molecular Pharmaceutics, 4*(6), 807–818. 10.1021/mp700113r.

Anantachaisilp, S., Smith, S. M., Treetong, A., Pratontep, S., Puttipipatkhachorn, S., & Ruktanonchai, U. R. (2010). Chemical and structural investigation of lipid nanoparticles: Drug-lipid interaction and molecular distribution. *Nanotechnology, 21*(12). 10.1088/0957-4484/21/12/125102.

Araujo, V. H. S., da Silva, P. B., Szlachetka, I. O., da Silva, S. W., Fonseca-Santos, B., Chorilli, M., et al. (2020). The influence of NLC composition on curcumin loading under a physicochemical perspective and in vitro evaluation. *Colloids and Surfaces A: Physicochemical and Engineering Aspects, 602*, Article 125070. 10.1016/j.colsurfa.2020.125070.

Bayés-García, L., Sato, K., & Ueno, S. (2020). Polymorphism of Triacylglycerols and Natural Fats. *Bailey's Industrial Oil and Fat Products*, 1–49. 10.1002/047167849x.bio020.pub2.

Bondì, M. L., Emma, M. R., Botto, C., Augello, G., Azzolina, A., Di Gaudio, F., et al. (2017). Biocompatible Lipid Nanoparticles as Carriers to Improve Curcumin Efficacy in Ovarian Cancer Treatment. *Journal of Agricultural and Food Chemistry, 65*(7), 1342–1352. 10.1021/acs.jafc.6b04409.

Borges, A., de Freitas, V., Mateus, N., Fernandes, I., & Oliveira, J. (2020). Solid lipid nanoparticles as carriers of natural phenolic compounds. *Antioxidants, 9*(10), 998. 10.3390/antiox9100998.

Bose, S., Du, Y., Takhistov, P., & Michniak-Kohn, B. (2013). Formulation optimization and topical delivery of quercetin from solid lipid based nanosystems. *International Journal of Pharmaceutics, 441*(1–2), 56–66. 10.1016/j.ijpharm.2012.12.013.

Brubach, J. B., Jannin, V., Mahler, B., Bourgaux, C., Lessieur, P., Roy, P., & Ollivon, M. (2007). Structural and thermal characterization of glyceryl behenate by X-ray diffraction coupled to differential calorimetry and infrared spectroscopy. *International Journal of Pharmaceutics, 336*(2), 248–256. 10.1016/j.ijpharm.2006.11.057.

Bunjes, H., Westesen, K., & Koch, M. H. J. (1996). Crystallization tendency and polymorphic transitions in triglyceride nanoparticles. *International Journal of Pharmaceutics, 129*(1–2), 159–173. 10.1016/0378-5173(95)04286-5.

Bunjes, H., Drechsler, M., Koch, M. H. J., & Westesen, K. (2001). Incorporation of the model drug ubidecarenone into solid lipid nanoparticles. *Pharmaceutical Research, 18*, 287–293. 10.1023/A:1011042627714.

Bunjes, H., Koch, M. H. J., & Westesen, K. (2002). Effects of surfactants on the crystallization and polymorphism of lipid nanoparticles. In Lagaly G. *(eds) Molecular Organisation on Interfaces. Progress in Colloid and Polymer Science* (Vol. 121). Springer, Berlin, Heidelberg. https://doi.org/10.1007/3-540-47822-1_2.

Bunjes, H., & Unruh, T. (2007). Characterization of lipid nanoparticles by differential scanning calorimetry, X-ray and neutron scattering. *Advanced Drug Delivery Reviews, 59*(6), 379–402. 10.1016/j.addr.2007.04.013.

Bunjes, H. (2010). Lipid nanoparticles for the delivery of poorly water-soluble drugs. *Journal of Pharmacy and Pharmacology, 62*(11), 1637–1645. 10.1111/j.2042-7158.2010.01024.x.

Canselier, J. P., Delmas, H., Wilhelm, A. M., & Abismaïl, B. (2001). Ultrasound emulsification - An overview. *Journal of Dispersion Science and Technology, 23*(1–3), 333–349. 10.1080/01932690208984209.

Cirri, M., Maestrini, L., Maestrelli, F., Mennini, N., Mura, P., Ghelardini, C., & Mannelli, L. D. C. (2018). Design, characterization and in vivo evaluation of nanostructured lipid carriers (NLC) as a new drug delivery system for hydrochlorothiazide oral administration in pediatric therapy. *Drug Delivery, 25*(1), 1910–1921. 10.1080/10717544.2018.1529209.

Das, S., & Chaudhury, A. (2011a). Recent advances in lipid nanoparticle formulations with solid matrix for oral drug delivery. *AAPS PharmSciTech, 12*(1), 62–76. 10.1208/s12249-010-9563-0.

Das, S., Ng, W. K., Kanaujia, P., Kim, S., & Tan, R. B. H. (2011b). Formulation design, preparation and physicochemical characterizations of solid lipid nanoparticles containing a hydrophobic drug: Effects of process variables. *Colloids and Surfaces B: Biointerfaces, 88*(1), 483–489. 10.1016/j.colsurfb.2011.07.036.

Doktorovova, S., Souto, E. B., & Silva, A. M. (2017). Hansen solubility parameters (HSP) for prescreening formulation of solid lipid nanoparticles (SLN): in vitro testing of curcumin-loaded SLN in MCF-7 and BT-474 cell lines. *Pharmaceutical Development and Technology, 23*(1), 96–105. 10.1080/10837450.2017.1384491.

Espinosa-Olivares, M. A., Delgado-Buenrostro, N. L., Chirino, Y. I., Trejo-Márquez, M. A., Pascual-Bustamante, S., & Ganem-Rondero, A. (2020). Nanostructured lipid carriers loaded with curcuminoids: Physicochemical characterization, in vitro release, ex vivo skin penetration, stability and antioxidant activity. *European Journal of Pharmaceutical Sciences, 155*, Article 105533. 10.1016/j.ejps.2020.105533.

Fang, J. Y., Fang, C. L., Liu, C. H., & Su, Y. H. (2008). Lipid nanoparticles as vehicles for topical psoralen delivery: Solid lipid nanoparticles (SLN) versus nanostructured lipid carriers (NLC). *European Journal of Pharmaceutics and Biopharmaceutics, 70*(2), 633–640. 10.1016/j.ejpb.2008.05.008.

Freitas, C., & Müller, R. H. (1998). Effect of light and temperature on zeta potential and physical stability in solid lipid nanoparticle (SLN®) dispersions. *International Journal of Pharmaceutics, 168*, 221–229. 10.1016/S0378-5173(98)00092-1.

Freitas, C., & Müller, R. H. (1999). Correlation between long-term stability of solid lipid nanoparticles (SLN(TM)) and crystallinity of the lipid phase. *European Journal of Pharmaceutics and Biopharmaceutics, 47*(2), 125–132. 10.1016/S0939-6411(98)00074-5.

Gokce, E. H., Korkmaz, E., Dellera, E., Sandri, G., Cristina Bonferoni, M., & Ozer, O (2012). Resveratrol-loaded solid lipid nanoparticles versus nanostructured lipid carriers: Evaluation of antioxidant potential for dermal applications. *International Journal of Nanomedicine, 7*, 1841–1850. 10.2147/IJN.S29710.

Gupta, R., & Rousseau, D. (2012). Surface-active solid lipid nanoparticles as Pickering stabilizers for oil-in-water emulsions. *Food and Function*, 3, 302–311. https://doi.org/10.1039/c2fo10203j.

Hamdani, J., Moës, A. J., & Amighi, K. (2003). Physical and thermal characterisation of Precirol® and Compritol® as lipophilic glycerides used for the preparation of controlled-release matrix pellets. *International Journal of Pharmaceutics, 260*(1), 47–57. 10.1016/S0378-5173(03)00229-1.

Hansen, C. M. (2007). Hansen solubility parameters: A user's handbook: Second edition. *Hansen Solubility Parameters: A Users Handbook, Second Edition* (2nd ed.). CRC Press. 10.1201/9781420006834.

Helgason, T., Awad, T. S., Kristbergsson, K., McClements, D. J., & Weiss, J. (2009). Effect of surfactant surface coverage on formation of solid lipid nanoparticles (SLN). *Journal of Colloid and Interface Science, 334*(1), 75–81. 10.1016/j.jcis.2009.03.012.

Hu, F. Q., Jiang, S. P., Du, Y. Z., Yuan, H., Ye, Y. Q., & Zeng, S. (2005). Preparation and characterization of stearic acid nanostructured lipid carriers by solvent diffusion method in an aqueous system. *Colloids and Surfaces B: Biointerfaces, 45*(3–4), 167–173. 10.1016/j.colsurfb.2005.08.005.

Hu, L., Tang, X., & Cui, F. (2010). Solid lipid nanoparticles (SLNs) to improve oral bioavailability of poorly soluble drugs. *Journal of Pharmacy and Pharmacology, 56*(12), 1527–1535. 10.1211/0022357044959.

Jaiswal, P., Gidwani, B., & Vyas, A. (2016). Nanostructured lipid carriers and their current application in targeted drug delivery. *Artificial Cells, Nanomedicine and Biotechnology, 44*(1), 27–40. 10.3109/21691401.2014.909822.

Jenning, V., Schäfer-Korting, M., & Gohla, S. (2000a). Vitamin A-loaded solid lipid nanoparticles for topical use: Drug release properties. *Journal of Controlled Release, 66*(2–3), 115–126. 10.1016/S0168-3659(99)00223-0.

Jenning, V., Thünemann, A. F., & Gohla, S. H. (2000b). Characterisation of a novel solid lipid nanoparticle carrier system based on binary mixtures of liquid and solid lipids. *International Journal of Pharmaceutics, 199*(2), 167–177. 10.1016/S0378-5173(00)00378-1.

Jia, L. J., Zhang, D. R., Li, Z. Y., Feng, F. F., Wang, Y. C., Dai, W. T., et al. (2010). Preparation and characterization of silybin-loaded nanostructured lipid carriers. *Drug Delivery, 17*(1), 11–18. 10.3109/10717540903431586.

Jores, K., Mehnert, W., & Mäder, K. (2003). Physicochemical investigations on solid lipid nanoparticles and on oil-loaded solid lipid nanoparticles: A nuclear magnetic resonance and electron spin resonance study. *Pharmaceutical Research, 20*, 1274–1283. 10.1023/A:1025065418309.

Jores, K., Mehnert, W., Drechsler, M., Bunjes, H., Johann, C., & Mäder, K. (2004). Investigations on the structure of solid lipid nanoparticles (SLN) and oil-loaded solid lipid nanoparticles by photon correlation spectroscopy, field-flow fractionation and transmission electron microscopy. *Journal of Controlled Release, 95*(2), 217–227. 10.1016/j.jconrel.2003.11.012.

Kasongo, K. W., Pardeike, J., Müller, R. H., & Walker, R. B. (2011a). Selection and characterization of suitable lipid excipients for use in the manufacture of didanosine-loaded solid lipid nanoparticles and nanostructured lipid carriers. *Journal of Pharmaceutical Sciences, 100*(12), 5185–5196. 10.1002/jps.22711.

Kasongo, K. W., Shegokar, R., Müller, R. H., & Walker, R. B. (2011b). Formulation development and in vitro evaluation of didanosine-loaded nanostructured lipid carriers for the potential treatment of AIDS dementia complex. *Drug Development and Industrial Pharmacy, 37*(4), 396–407. 10.3109/03639045.2010.516264.

Kentish, S., Wooster, T. J., Ashokkumar, M., Balachandran, S., Mawson, R., & Simons, L. (2008). The use of ultrasonics for nanoemulsion preparation. *Innovative Food Science and Emerging Technologies*, 9(2), 170–175. https://doi.org/10.1016/j.ifset.2007.07.005.

Khan, S., Baboota, S., Ali, J., Khan, S., Narang, R. S., & Narang, J. K. (2015). Nanostructured lipid carriers: An emerging platform for improving oral bioavailability of lipophilic drugs. *International Journal of Pharmaceutical Investigation, 5*(4), 182–191. 10.4103/2230-973X.167661.

Khan, S., Minhas, M. U., Ahmad, M., & Sohail, M. (2017). Self-assembled supramolecular thermoreversible β-cyclodextrin/ethylene glycol injectable hydrogels with difunctional Pluronic®127 as controlled delivery depot of curcumin. Development, characterization and in vitro evaluation. *Journal of Biomaterials Science, 29*(1), 1–34 *Polymer Edition*. 10.1080/09205063.2017.1396707.

Kovacevic, A., Savic, S., Vuleta, G., Müller, R. H., & Keck, C. M. (2011). Polyhydroxy surfactants for the formulation of lipid nanoparticles (SLN and NLC): Effects on size, physical stability and particle matrix structure. *International Journal of Pharmaceutics, 406*(1–2), 163–172. 10.1016/j.ijpharm.2010.12.036.

Kovačević, A. B., Müller, R. H., & Keck, C. M. (2020). Formulation development of lipid nanoparticles: Improved lipid screening and development of tacrolimus loaded nanostructured lipid carriers (NLC). *International Journal of Pharmaceutics, 576*, Article 118918. 10.1016/j.ijpharm.2019.118918.

Kumar, R., Singh, A., Garg, N., & Siril, P. F. (2018). Solid lipid nanoparticles for the controlled delivery of poorly water soluble non-steroidal anti-inflammatory drugs. *Ultrasonics Sonochemistry, 40*(Pt A), 686–696. 10.1016/j.ultsonch.2017.08.018.

Lee, W.-H., Loo, C.-Y., Bebawy, M., Luk, F., Mason, R., & Rohanizadeh, R. (2013). Curcumin and its Derivatives: Their Application in Neuropharmacology and Neuroscience in the 21st Century. *Current Neuropharmacology, 11*(4), 338–378. 10.2174/1570159x11311040002.

Lim, H., Jo, M., Ban, C., & Choi, Y. J. (2020). Interfacial and colloidal characterization of oil-in-water emulsions stabilized by interface-tunable solid lipid nanoparticles. *Food Chemistry, 306*, Article 125619. 10.1016/j.foodchem.2019.125619.

Makoni, P. A., Kasongo, K. W., & Walker, R. B. (2019). Short term stability testing of efavirenz-loaded solid lipid nanoparticle (SLN) and nanostructured lipid carrier (NLC) dispersions. *Pharmaceutics, 397*(8), 11. 10.3390/pharmaceutics11080397.

Makoni, P. A., Ranchhod, J., Kasongo, K. W., Khamanga, S. M., & Walker, R. B. (2020). The use of quantitative analysis and Hansen solubility parameter predictions for the selection of excipients for lipid nanocarriers to be loaded with water soluble and insoluble compounds. *Saudi Pharmaceutical Journal, 28*(3), 308–315. 10.1016/j.jsps.2020.01.010.

Müller, R. H., Mäder, K., & Gohla, S. (2000). Solid lipid nanoparticles (SLN) for controlled drug delivery - A review of the state of the art. *European Journal of Pharmaceutics and Biopharmaceutics, 50*(1), 161–177. 10.1016/S0939-6411(00)00087-4.

Müller, R. H., Radtke, M., & Wissing, S. A. (2002). Nanostructured lipid matrices for improved microencapsulation of drugs. *International Journal of Pharmaceutics, 242*(1–2), 121–128. 10.1016/S0378-5173(02)00180-1.

Norton, I. T., Lee-Tuffnell, C. D., Ablett, S., & Bociek, S. M. (1985). A calorimetric, NMR and X-ray diffraction study of the melting behavior of tripalmitin and tristearin and their mixing behavior with triolein. *Journal of the American Oil Chemists' Society, 62*(8), 1237–1244. 10.1007/BF02541834.

Nnamani, P. O., Hansen, S., Windbergs, M., & Lehr, C. M. (2014). Development of artemether-loaded nanostructured lipid carrier (NLC) formulation for topical application. *International Journal of Pharmaceutics, 477*(1–2), 208–217. 10.1016/j.ijpharm.2014.10.004.

Obinu, A., Porcu, E. P., Piras, S., Ibba, R., Carta, A., Molicotti, P., et al. (2020). Solid lipid nanoparticles as formulative strategy to increase oral permeation of a molecule active in multidrug-resistant tuberculosis management. *Pharmaceutics, 12*(12), 1132. 10.3390/pharmaceutics12121132.

Oehlke, K., Behsnilian, D., Mayer-Miebach, E., Weidler, P. G., & Greiner, R. (2017). Edible solid lipid nanoparticles (SLN) as carrier system for antioxidants of different lipophilicity. *PLoS ONE, 12*(2), Article e0171662. 10.1371/journal.pone.0171662.

Pawlik, A., Kurukji, D., Norton, I., & Spyropoulos, F. (2016). Food-grade Pickering emulsions stabilised with solid lipid particles. *Food and Function*, 7(6), 2712–2721. https://doi.org/10.1039/c6fo00238b.

Perez, M. (2005). Gibbs-Thomson effects in phase transformations. *Scripta Materialia, 52*(8), 709–712. 10.1016/j.scriptamat.2004.12.026.

Pivette, P., Faivre, V., Brubach, J. B., Daste, G., Ollivon, M., & Lesieur, S. (2014). Polymorphism of glyceryl behenates: From the individual compounds to the pharmaceutical excipient. *Chemistry and Physics of Lipids*, 183, 191–203. https://doi.org/10.1016/j.chemphyslip.2014.07.005.

Pouton, C. W. (2006). Formulation of poorly water-soluble drugs for oral administration: Physicochemical and physiological issues and the lipid formulation classification system. *European Journal of Pharmaceutical Sciences, 29*(3–4), 278–287. 10.1016/j.ejps.2006.04.016.

Reitz, C., & Kleinebudde, P. (2007). Influence of thermal and thermo-mechanical treatment : CCComparison of two lipids with respect to their suitability for solid lipid extrusion. *Journal of Thermal Analysis and Calorimetry, 89*(3), 669–673. 10.1007/s10973-006-7953-z.

Riddick, T. M. (1968). *Control of colloid stability through zeta potential: with a closing chapter on Its Relationship to Cardiovascular Disease*. Zeta-Meter, Inc.

Rousseau, D. (2000). Fat crystals and emulsion stability - A review. *Food Research International, 33*(1), 3–14. 10.1016/S0963-9969(00)00017-X.

Sakellari, G. I., Zafeiri, I., Pawlik, A., Kurukji, D., Taylor, P., Norton, I. T., & Spyropoulos, F. (2021). Independent co-delivery of model actives with different degrees of hydrophilicity from oil-in-water and water-in-oil emulsions stabilised by solid lipid particles via a Pickering mechanism: a-proof-of-principle study. *Journal of Colloid and Interface Science, 587*, 644–649. 10.1016/j.jcis.2020.11.021.

Sapino, S., Carlotti, M. E., Pelizzetti, E., Vione, D., Trotta, M., & Battaglia, L. (2005). Protective effect of SLNs encapsulation on the photodegradation and thermal degradation of retinyl palmitate introduced in hydroxyethylcellulose gel. *Journal of Drug Delivery Science and Technology, 15*(2), 159–165. 10.1016/s1773-2247(05)50021-2.

Sato, K. (2001). Crystallization behaviour of fats and lipids - A review. *Chemical Engineering Science, 56*(7), 2255–2265. 10.1016/S0009-2509(00)00458-9.

Schröder, A., Sprakel, J., Schroën, K., & Berton-Carabin, C. C. (2017). Tailored microstructure of colloidal lipid particles for Pickering emulsions with tunable properties. *Soft Matter, 13*(17), 3190–3198. 10.1039/c6sm02432g.

Schröder, A., Laguerre, M., Sprakel, J., Schroën, K., & Berton-Carabin, C. C. (2020). Pickering particles as interfacial reservoirs of antioxidants. *Journal of Colloid and Interface Science, 575*, 489–498. 10.1016/j.jcis.2020.04.069.

Scomoroscenco, C., Teodorescu, M., Raducan, A., Stan, M., Voicu, S. N., Trica, B., Ninciuleanu, C. M., Nistor, C. L., Mihaescu, C. I., Petcu, C., & Cinteza, L. O. (2021). Novel gel microemulsion as topical drug delivery system for curcumin in dermatocosmetics. *Pharmaceutics, 13*(4), 505. 10.3390/pharmaceutics13040505.

Severino, P., Pinho, S. C., Souto, E. B., & Santana, M. H. A. (2011). Crystallinity of Dynasan ®114 and Dynasan ®118 matrices for the production of stable Miglyol ®-loaded nanoparticles. *Journal of Thermal Analysis and Calorimetry, 108*, 101–108. 10.1007/s10973-011-1613-7.

Severino, P., Andreani, T., Macedo, A. S., Fangueiro, J. F., Santana, M. H. A., Silva, A. M., & Souto, E. B. (2012). Current State-of-Art and New Trends on Lipid Nanoparticles (SLN and NLC) for Oral Drug Delivery. Journal of Drug Delivery, 2012*, 750891*. 10.1155/2012/750891.

Shah, M., & Agrawal, Y. (2012). Ciprofloxacin hydrochloride-loaded glyceryl monostearate nanoparticle: Factorial design of Lutrol F68 and Phospholipon 90G. *Journal of Microencapsulation, 29*(4), 331–343. 10.3109/02652048.2011.651498.

Shah, M., Agrawal, Y. K., Garala, K., & Ramkishan, A. (2012). Solid lipid nanoparticles of a water soluble drug, ciprofloxacin hydrochloride. *Indian Journal of Pharmaceutical Sciences, 74*(5), 434–442. 10.4103/0250-474X.108419.

Shah, M., & Agrawal, Y. (2013). High throughput screening: an in silico solubility parameter approach for lipids and solvents in SLN preparations. *Pharmaceutical Development and Technology, 18*(3), 582–590. 10.3109/10837450.2011.635150.

Sharifi-Rad, J., Rayess, Y. El, Rizk, A. A., Sadaka, C., Zgheib, R., Zam, W., et al. (2020). Turmeric and Its Major Compound Curcumin on Health: Bioactive Effects and Safety Profiles for Food, Pharmaceutical, Biotechnological and Medicinal Applications. *Frontiers in Pharmacology, 11*, 01021. 10.3389/fphar.2020.01021.

Souto, E. B., Wissing, S. A., Barbosa, C. M., & Müller, R. H. (2004a). Development of a controlled release formulation based on SLN and NLC for topical clotrimazole delivery. *International Journal of Pharmaceutics, 278*(1), 71–77. 10.1016/j.ijpharm.2004.02.032.

Souto, E. B., Wissing, S. A., Barbosa, C. M., & Müller, R. H. (2004b). Evaluation of the physical stability of SLN and NLC before and after incorporation into hydrogel formulations. *European Journal of Pharmaceutics and Biopharmaceutics, 58*(1), 83–90. 10.1016/j.ejpb.2004.02.015.

Souto, E. B., & Müller, R. H. (2005). SLN and NLC for topical delivery of ketoconazole. *Journal of Microencapsulation, 22*(5), 501–510. 10.1080/02652040500162436.

Souto, E. B., Mehnert, W., & Müller, R. H. (2006). Polymorphic behaviour of Compritol®888 ATO as bulk lipid and as SLN and NLC. *Journal of Microencapsulation, 23*(4), 417–433. 10.1080/02652040600612439.

Sutananta, W., Craig, D. Q. M., & Newton, J. M. (1994). The effects of ageing on the thermal behaviour and mechanical properties of pharmaceutical glycerides. *International Journal of Pharmaceutics, 111*(1), 51–62. 10.1016/0378-5173(94)90401-4.

Tamjidi, F., Shahedi, M., Varshosaz, J., & Nasirpour, A. (2014). Design and characterization of astaxanthin-loaded nanostructured lipid carriers. *Innovative Food Science and Emerging Technologies*, 26, 366–374. https://doi.org/10.1016/j.ifset.2014.06.012.

Tan, T. B., Chu, W. C., Yussof, N. S., Abas, F., Mirhosseini, H., Cheah, Y. K., … Tan, C. P. (2016). Physicochemical, morphological and cellular uptake properties of lutein nanodispersions prepared by using surfactants with different stabilizing mechanisms. *Food and Function*, 7(4), 2043–2051. https://doi.org/10.1039/c5fo01621e.

Van Krevelen, D. W., & Te Nijenhuis, K. (2009). Chapter 7 - Cohesive Properties and Solubility in Properties of Polymers. In *Properties of Polymers* (pp. 189–227). Amsterdam: Elsevier. 10.1016/b978-0-08-054819-7.00007-8.

Van Malssen, K., Peschar, R., Brito, C., & Schenk, H. (1996). Real-time X-ray powder diffraction investigations on cocoa butter. III. Direct β-crystallization of cocoa butter: Occurrence of a memory effect. *JAOCS, Journal of the American Oil Chemists' Society, 73*, 1225–1230. 10.1007/BF02525450.

Wang, W., Chen, T., Xu, H., Ren, B., Cheng, X., Qi, R., et al. (2018). Curcumin-loaded solid lipid nanoparticles enhanced anticancer efficiency in breast cancer. *Molecules, 23*(7), 1578. 10.3390/molecules23071578.

Weiss, J., Decker, E. A., McClements, D. J., Kristbergsson, K., Helgason, T., & Awad, T. (2008). Solid lipid nanoparticles as delivery systems for bioactive food components. *Food Biophysics, 3*, 146–154. 10.1007/s11483-008-9065-8.

Westesen, K., Bunjes, H., & Koch, M. H. J. (1997). Physicochemical characterization of lipid nanoparticles and evaluation of their drug loading capacity and sustained release potential. *Journal of Controlled Release, 48*(2–3), 223–236. 10.1016/S0168-3659(97)00046-1.

Wolska, E., Sznitowska, M., Krzemińska, K., & Monteiro, M. F. (2020). Analytical techniques for the assessment of drug-lipid interactions and the active substance distribution in liquid dispersions of solid lipid microparticles (SLM) produced de novo and reconstituted from spray-dried powders. *Pharmaceutics, 12*(7), 664. 10.3390/pharmaceutics12070664.

Yoshino, H., Kobayashi, M., & Samejima, M. (1982). Influence of the Liquid Phase Coexisting in Fatty Suppository Bases on the Polymorphic Transition Rate. *Chemical and Pharmaceutical Bulletin, 30*(8), 2941–2950. 10.1248/cpb.30.2941.

Zafeiri, I., Norton, J. E., Smith, P., Norton, I. T., & Spyropoulos, F. (2017a). The role of surface active species in the fabrication and functionality of edible solid lipid particles. *Journal of Colloid and Interface Science, 500*, 228–240. 10.1016/j.jcis.2017.03.085.

Zafeiri, I., Smith, P., Norton, I. T., & Spyropoulos, F. (2017b). Fabrication, characterisation and stability of oil-in-water emulsions stabilised by solid lipid particles: The role of particle characteristics and emulsion microstructure upon Pickering functionality. *Food and Function, 8*(7), 2583–2591. 10.1039/c7fo00559h.

Zimmermann, E., Souto, E. B., & Müller, R. H. (2005). Physicochemical investigations on the structure of drug-free and drug-loaded solid lipid nanoparticles (SLN^{TM}) by means of DSC and 1H NMR. *Pharmazie, 60*(7), 508–513.

Zoubari, G., Staufenbiel, S., Volz, P., Alexiev, U., & Bodmeier, R. (2017). Effect of drug solubility and lipid carrier on drug release from lipid nanoparticles for dermal delivery. *European Journal of Pharmaceutics and Biopharmaceutics, 110*, 39–46. 10.1016/j.ejpb.2016.10.021.

Zur Mühlen, A., Schwarz, C., & Mehnert, W. (1998). Solid lipid nanoparticles (SLN) for controlled drug delivery - Drug release and release mechanism. *European Journal of Pharmaceutics and Biopharmaceutics, 45*(2), 149–155. 10.1016/S0939-6411(97)00150-1.